Reply to Reviewer 1

We thank the Reviewer for the positive evaluation of the manuscript and the good comments. In the following, we address all comments and questions raised (Reviewer's comments in italics). Text changes in the manuscript are highlighted in color (except minor wording changes).

General comments:

I think that the apparent step-change extratropical in age around the early-mid 1990s is an interesting result and one of the clearer differences between ERA5 and ERA-Interim. The fact that this does not appear clearly in observational data (e.g. Fig. 10) may bring into question the reliability of ERA5 trends. Its also interesting that this step-change is not apparent in the tropical upwelling (Diallo et al. 2020, their Fig 12). I might encourage the authors to elaborate a little more on this in the paper as the result is not very prominent. In particular, do any TEM diagnostics of the circulation show this step change, or is this only seen in age calculations? Is so, could the authors speculate as to why? If this step-change is not thought to be real, do the authors have any suggestions for what change in the assimilation scheme may be responsible?

This is indeed a very good question - and not easy to answer. At first glance, the change in age of air in the mid-nineties appears as a sudden step-change, but a closer look shows that the change occurs over a few years, between about 1991-1995. This change is clearly evident in ERA5 age, and to a weaker degree also seen in ERA-Interim. The age time series in Fig. 9 show that the clearer step change in ERA5 in the mid-nineties is mainly a result of the positive age trend in the eighties and the age increase around 1991 which is likely related to the Pinatubo aerosol. The main difference to ERA-Interim is the trend over the eighties.
As suggested by the Reviewer, we further investigated basic meteorological variables for similar changes, and we considered both the residual circulation vertical velocity and the diabatic heating rate (new Fig. 12 in the revised manuscript). At upper stratospheric levels the heating rates show abrupt changes related to changes in the assimilation system (e.g., in 1998), as discussed for ERA-Interim e.g. by Abalos et al. (2015). However, in the lower stratosphere none of the two variables shows a step-like change in the mid-nineties which could be related to the age of air change. On the other hand, the heating rates show a decrease after the Pinatubo eruption (1991) in both reanalysis, related to the age increase during the same period. The difference in the strength of this effect between the two reanalysis, and also between heating rates and residual circulation velocity, are not clear to us.
We agree with the Reviewer that a more thorough discussion of these issues clearly improves the paper and we included a new figure (Fig. 12) showing the vertical velocity and heating rate changes and extended the discussion section 6 in this regard.

Minor and Technical comments:

L7: *Above: it wasnt clear to me what this was referring to as being above. Maybe in the mid-upper stratosphere would be clearer?*
Indeed, our wording here was not precise. We actually meant that ERA5 age appears somewhat high-biased outside the TTL at all locations where we compared to observations. However, we compared only at 20km (aircraft data, Fig. 10a), in NH middle latitudes above 24km (balloon data, Fig. 10b), and in the NH lower stratosphere between about 350-480K (aircraft and balloon data, Fig. 11). Hence, this statement should not be considered as too strong. To be more precise, we changed the wording to: "At 20 km and in the NH stratosphere, ERA5 age values are at the upper edge of the uncertainty range from tracer observations, indicating a comparatively slow BDC." Note that we also changed parts of the comparison to observations in Sect. 5, as suggested by Reviewer 2 (we replaced the age-F11 correlation analysis with an analysis of the age difference distributions between model and observations).

L94: *theta (potential temperature) should be defined.*
Sentence has been changed accordingly.

L105: *along → along with?*
We just deleted "along".

Fig. 2: *I think this would benefit if a difference plot were also shown (ERA-Int minus ERA5) to aid with comparison of the two reanalyses and with Fig 1 e-g. It is quite difficult to pick out the differences without such a plot.*
Thanks for this suggestion, which eases the comparison! We just added difference plots to all cases (ERA5 and ERA-Interim, DJF and JJA) in Figs. 1 and 2.

Fig. 3: *This is a minor point, but I would encourage the authors to consider using a perceptually uniform color scale for the age plots (a,b,d,e), such as grayscale, viridis etc. The rainbow scheme used here can introduce the appearance of false boundaries (where the yellow color are) in the date. The same goes for Figs 4 and 5.*
We agree that the used color scheme could probably be improved. However, most publications we are aware of show age of air usig a similar blue–green–red color scheme. As readers therefore are mostly used to that we would stay with it here.

L391: *strongly overly. Im not sure what this means? Perhaps decadal variations are significant compared to potential long-term trends?*
We changed the sentence as suggested.

L427: *steplike change around the year 2000: To me it looks like the main steplike change in ERA5 is over 1992-1997 rather than around 2000.*
This is totally correct, and the “2000” was just wrong - Thanks for pointing this out! We changed the text to “in the mid-nineties”.

Reply to Reviewer 2

We thank the Reviewer Simon Chabrillat for the very careful review, the many detailed comments, and the generally positive evaluation of the manuscript. In the following, we address all comments and questions raised (Reviewer's comments in italics). Text changes in the manuscript are highlighted in color (except minor wording changes).

General comments:

The representation of the BDC and its time variations in reanalyses is an important topic for modellers of atmospheric composition in the middle atmosphere, and ERA-5 is set to become as broadly used as ERA-Interim has been for the twelve last years. Hence this study is of high interest and very timely for ACP. The modelling tools are very well tailored for these aims, and the modelling experiments are well designed. The manuscript is well structured and well written. All my comments deal with the description of the methods and observations, and the interpretation of the results. Hence I recommend publication of the paper after a minor revision (i.e. no additional calculations should be necessary).
In my opinion the manuscript comes short in the comparisons with trace gas observations (section 5). These suggest that the diabatic Age of Air (AoA) is overestimated in ERA-5, at least in the lower stratosphere at most latitudes (for some unspecified time period; Fig. 10a) and also in the middle-latitudes during the first half of the 1990s (Fig. 10b). It is repeatedly stated that the ERA-5 results are at the upper margin of the observational uncertainty range but these observational uncertainties are not clearly described in Figures 10 and 11, preventing a serious assessment of the significance of the apparent high bias using ERA-5. The AoA overestimation is confirmed by correlations between AoA and CFC-11, using as reference a campaign of aircraft observations (Fig. 11) but here also there is no indication of the observational uncertainties. These comparisons are briefly discussed in section 6 (lines 355-360) but mainly to tone down their importance and to avoid overinterpretation. The authors seem so unsure about these comparisons that they completely overlooked section 5 in the abstract.
It is well understood that these comparisons are not certain and that the same team is preparing a deeper investigation. Yet the results already shown in this manuscript are clearly of high interest for all readers and should be treated with due care. I recommend to better explain the observational uncertainties (see specific comments SC25 and SC26 below) and spend more effort to assess the significance of the overestimations of AoA by ERA-5 (see specific comment SC29 below). The abstract should highlight the results of section 5, and of course mention the discussion about their significance.

We agree that the submitted manuscript did not present a too detailed comparison between model and observations and that this part could be further improved. However, as the Reviewer already recognized, we can not give too strong conclusions due to the scarcity of available observational data and their uncertainty. In the revised manuscript, we follow the Reviewer's suggestions and included (1) a more detailed description and discussion of the observational uncertainties, and (2) a clearer comparison of model age of air to Geophysica in-situ observations, as explained in detail in the following:

(1) Section 5 now includes more details on the observations by Engel et al. (2017), Laube et al. (2020), and those compiled by Waugh and Hall (2002). As the Waugh and Hall (2002) data set represents a standard benchmark for model evaluation, and has been used by many other authors before (e.g., Diallo et al., 2012; Chabrillat et a., 2018; Ploeger et al., 2019) we just added a few more details, like the period (1992–1997) and data type (ER–2 aircraft observations), and refer clearly to the Waugh and Hall publication. Furthermore, we used this data set as a benchmark for the model climatology, although the data are only from the nineties. However, similar comparisons to model climatologies have been made in many other studies (e.g., Diallo et al., 2012; Chabrillat et a., 2018; Ploeger et al., 2019). We included a short note on these issues in Sect. 5.
Also the data by Engel et al. (2017) have been well described in the literature (Engel et al., 2009, 2017). We mainly added a short description on the uncertainty, which is related to the sampling (representativeness), tropospheric mixing ratios, the used age spectrum parameterization and the absolute measurement error.
The data by Laube et al. (2020) is the newest data set and we added more details here, although also these data are already well described in the above mentioned paper. We now emphasize that these data are from 5 aircraft measurement campaigns with the Geophysica high-altitude research aircraft during 2009–2017. In particular, we added an analysis and description of the observational uncertainty, leading to an overall uncertainty range of ± 0.78 years (see Sect. 5).

(2) We agree that the comparison in terms of correlations was somewhat complicated and not clear regarding the uncertainty ranges. We entirely changed this part of the paper. Instead of the correlations, in the revised version we just compare mean age of air. The new Fig. 11 presents the mean age model bias in terms of distributions of the differences model minus observations. The estimated overall uncertainty range for the ob-

servations (see point 1, above) allows assessing what fraction of data points are outside this uncertainty range. The fraction outside the uncertainty range is 21% for ERA–Interim and 56% for ERA5. Hence, ERA5 indeed appears somewhat high-biased. However, the 1-σ ranges of the mean model bias and the observational uncertainty overlap (see Fig. 11), such that the bias is not significant at 66% confidence level. The related discussion in Sect. 5 and in the discussion is entirely rewritten and improved. Thanks for this very good suggestion which clearly improves and clarifies the paper!

Major comments:

MC1. *The introduction and the discussion draw an often-stated parallel between the decreasing AoA found by some reanalyses in some hemispheres during some periods (maximum 30 years) and the decreasing AoA robustly found by most climate models over 100 years due to increasing greenhouse gases. The validity of this parallel is doubtful, as correctly noted in the discussion (lines 392-393): The 30-40 years time series is presumably still too short for computing long-term trends in reanalysis, where stratospheric variability might be larger compared to climate models. Fortunately this parallel is not necessary because AoA variations in the actual world over timescales of 1 to 3 decades are worth studying on their own. On this topic see also SC24 and SC31 below.*
We fully agree with the Reviewer that studying AoA variations over shorter than centennial time scales is interesting and important. But it is also of strong interest whether the climate model predicted trend can be seen already in the reanalysis over the last decades. We added some explanatory text in the discussion Sect. 6.

MC2. *Section 2.1 explains two changes in methodology with respect to the previous age of air studies by this team: the mean age is now computed from a separate clock-tracer (rather than as the first moment of the AoA spectra); and the vertical velocity is not corrected any more for missing balance in the cross-isentropic mass flux. While the impacts of these changes are briefly described in that section and mentioned in section 4, they are not shown in the paper. In view of the long and successful series of AoA studies relying on ClaMS, it is important to show the impact of these changes on mean AoA. The impact of the first change especially could easily be shown on some existing figures, e.g. adding dashed black lines on Fig. 4 and 5 to show mean AoA from clock-tracer calculations.*
It would be even more interesting to add a figure showing the Age spectrum for a given latitude and potential temperature. Ploeger et al. (2019) did precisely this in their Fig. 12a, showing clearly the importance of the spectrum tail in MERRA-2. In view of the apparent similarities between ERA-5 and MERRA-2 (when compared with ERA-I), this could be highly relevant here as well. Of course the mean AoA from the spectrum would also be compared with the mean AoA from the clock tracer.
We agree that it is important to quantify the uncertainties in the methodology. However, the difference between mean age calculated from the age spectrum and from a clock-tracer has been analysed in detail and presented for the same model set-up already by Ploeger and Birner (2016), their Figs. 4 and A1. We included a reference to this paper at the appropriate place in the methods section. Regarding the age spectrum comparison at a given latitude and potential temperature, we think that Figs. 4 and 5 already present exactly this information, even for all latitudes at 400 and 600 K. As the paper includes already 12 figures we refrain from adding an additional line plot, which would just double already existing information.

MC3. *Section 2 lacks a (short) description of the linear regression approach used for section 4: when de-seasonalized time series are regressed, do the linear regressions use climate proxies such as QBO, ENSO, volcanic forcings? If yes, what are the proxies actually used? The regression method also provides standard deviations that are used to assess the significance of the regressed trends (fig. 6). While this is standard, it remains important to explain how these standard deviations are ovtained (in a few words and with a reference).*
We used just a simple linear regression of deseasonalized time series (after subtracting the mean annual cycle), hence without subtraction of variability related to e.g. QBO or ENSO. This information was already provided in the submitted manuscript at the beginning of Sect. 4, where the trends are presented and discussed. We tried to further clarify the wording of this paragraph and added information on the significance of the calculated trends in the revised version.

MC4. *Section 2.2 states (lines 139-140): However, we maintain the full vertical resolution. Hence, the ERA5 data to drive the ClaMS model in this study has 137 hybrid ECMWF model levels, to compare with the ERAInterim 60 levels. How is it possible to maintain vertical resolution while going from sigma-pressure to sigma-theta? What is the actual vertical resolution in both simulations? The reader must get a sense that the ERA5 simulation makes full use of its increased vertical resolution. This is important as it certainly plays a role in the diabatic heating gap that is found at 350K (Fig. 1e) and repeatedly mentioned in the manuscript.*
As CLaMS is a Lagrangian transport model, the grid points are provided by air parcels which are irregularly distributed in space. Hence, meteorological data (e.g., winds) need to be interpolated onto the air parcel positions.

To maintain full reanalysis vertical resolution, this interpolation is done from fields on native model levels. In that sense, the input reanalysis data for CLaMS has the original reanalysis vertical resolution (137 levels for ERA5, 60 levels for ERA–Interim). We added information and tried to clarify the respective text in the methods section.

MC5. *According to Diallo et al. (2020), the vertical coordinate that is used for derivation of the residual vertical velocity $\overline{w}^*$ is log-pressure height, i.e. a constant-pressure grid assuming a scale height of 7 km. Yet Fig. 2 uses Altitude for the Y-axis. This is confusing and prevents matching the levels of Fig. 2 with the iso-pressure levels explicitly drawn of Fig. 1, 3, 6, 8. If the actual Y-axis for Fig. 2 is log-pressure height, I recommend to re-draw Fig. 2 with pressures on the (logarithmic) Y- axes.*
Sorry for not having been clear here! The vertical coordinate used for calculating residual circulation velocity here is indeed log-pressure altitude, as is the standard framework for Transformed Eulerian Mean computations. In the revised Fig. 2 we clearly state this in the caption.

MC6. *Fig. 8 compares the RCTT in ERA-5 and ERA-I, and the accompanying text states that Differences between mean age and RCTT are related to mixing effects. Yet the corresponding paragraph discusses only the changes in RCTT and does not attempt to disentangle the contributions of mixing and residual circulation to AoA and its time variations. In practice it is not possible to visually compare AoA (Fig. 3) and RCTT (Fig.8) because AoA is shown sparately for DJF and JJA while RCTT is shown as an annual mean (also the color maps differ).*
The goal with presenting the RCTTs is to discuss the pure residual circulation effect on stratospheric transit times. Indeed, these RCTTs can not be directly compared to mean age, therefore by purpose we chose different plotting styles and averaging periods. We added explanation and tried to clarify the paragraph explaining the differences between RCTTs and mean age in Sect. 4.

Specific comments:

SC1. *Line 10: ...changes in the assimilation system : reanalyses avoid any change in the assimilation system (i.e. the model and assimilation software); they suffer instead from changes in the observing system that is assimilated into the reanalysis. This formulation should be corrected throughout the manuscript.*
The formulation “assimilation system” was meant to also included the observational data. Nevertheless, to enhance clarity we changed the wording as suggested to “observations included in the assimilation system” throughout the manuscript.

SC2. *Lines 16 and 20 : The Brewer-Dobson circulation (BDC) is the global transport circulation in the stratosphere and The BDC is characterized by upwelling motion in the tropics, poleward transport in the stratosphere and downwelling above middle and high latitudes. While these characterizations are very common, they overlook the important branch of the BDC that extends into the mesosphere where it goes all the way from the summer pole to the winter pole (e.g. Fig.1, in Bnisch et al., 2011).*
A note on the mesospheric circulation branch is added.

SC3. *Lines 40-43: On the one hand, climate models ~~show~~ predict a robust strengthening and acceleration of the BDC with climate change (e.g., Butchart et al., 2010), manifesting in an increase in tropical upwelling and a decrease in global mean age of air. On the other hand... On what timescale does the climate model prediction appear? See MC1: the opposition between long-term AoA changes in climate models and multi-decadal AoA changes in reanalyses is misleading and not necessary.*
See our reply to MC1 above.

SC4. *Line 53: ...while inter-annual BDC variability seems to be well represented in reanalyses.... This statement should be more specific and have specific references because it is really not obvious to me, e.g. Chabrillat et al. (2018, Fig.10) found that the amplitude of the QBO impact on AoA can vary by a factor of 2 depending on the input reanalysis.*
The formulation has been specified, by removing the statement on “inter-annual variability” and focussing just on “decadal changes”.

SC5. *First paragraph of page 3: consider inserting here a reference to Fujiwara et al. (2017) as it is a general introduction of the reanalyses and their diversity, with a comprehensive description of the observing systems that they assimilate.*
A short note on S-RIP and the Fujiwara et al. (2017) paper is added.

SC6. *Lines 91-94: this paragraph should be expanded to introduce more smoothly diabatic transport and its advantages in the stratosphere (with references). It is espeecially important to define θ before it is used.*
We expanded the respective paragraph a bit (e.g., properly introducing θ, adding a reference), but not too

much, as we think the advantages of a diabatic transport formulation for the stratosphere are well-known. Too much discussion of these aspects here would rather distract the reader from the main points of the paper.

SC7. *Line 131: please provide a web link or reference to the ECMWF technical documentation for IFS CY41R2. The horizontal resolution is about 30km (T639): explain (in a few words) the spherical harmonics number.*
We just added another reference to the Hersbach et al. (2020) paper here, although it was already referenced at the end of the paragraph.

SC8. *Line 133: Simmons et al. (2020) describe the need for the ERA5.1 update and its differences with ERA5.0. It is really necessary to cite that reference here.*
Reference to Simmons et al. (2020) has been added.

SC9. *Line 138: what is the spectral truncature (wavenumber) corresponding to this 1x1 resolution? This is important to compare with the T639 number provided above.*
We did a transformation on-the-fly during the download as provided by the ECMWF MARS system, which is a direct transformation from T1279 to 1.0/1.0 degree, with an automatic truncation to T213. This is detailed now in the revised manuscript.

SC10. *Lines 141-146: For clarity, it is necessary to first explain in a few words what is the temperature tendency. Is the total diabatic heating rate Qtot the same quantity as the 5th temperature tendency provided by ERA, i.e. the mean temperature tendency due to [both? all?] parameterizations? Is Qtot nothing else than the sum of the temperature tendencies due to short-wave and long-wave parameterizations in all-sky conditions? Please clarify.*
Yes, the total diabatic heating rate (used here for driving CLaMS transport) is the 5th temperature tendency due to all parametrisations, including the mentioned radiative contributions, latent heat release, turbulent and sensitive heating. We added this information and clarified the text.

SC11. *$d\theta/dt$ is variously described in the text as the cross-isentropic vertical velocity (e.g. lines 145 and 163) or as the total diabatic heating rate (e.g. caption of Fig. 1). In view of Eq (3), I think that the second formulation is not rigorous. In any case the same formulation should be used consistently throughout the manuscript.*
Yes, the Reviewer is totally right with this comment that the vertical cross-isentropic velocity $\mathrm{d}\theta/\mathrm{d}t$ used for driving CLaMS transport is not exactly the reanalysis diabatic heating rate, but is calculated from the heating rate using Eq. 3. Actually, we already tried to use the wording carefully in the submitted manuscript, but as the comment shows with limited success. We went through the paper again and tried to further clarify the wording, such that when it is referred to the reanalysis quantity (or the driving quantity) we use "diabatic heating rate", when it is referred to the velocity used in CLaMS we use "diabatic (or cross-isentropic) vertical velocity". We hope this point is much clearer now.

SC12. *Line 166: Cross-isentropic tropical upwelling maximizes in boreal winter. But the equinox seasons are not shown or discussed anywhere, and it is problematic to write about tropical upwelling in boreal winter. Consider instead: Cross-isentropic tropical upwelling is larger in DJF than in JJA. This comment applies throughout the manuscript.*
We think it is frequently used wording in the literature to link "tropical upwelling maximum" to "boreal winter", as the upwelling seasonality is controlled by the hemispheric asymmetry in wave driving (stronger in the NH). Hence, we leave the formulations largely as they are, but checked again for consistency, and also included a short addition at first usage "boreal winter (December–February, DJF)".

SC13. *Line 170: ...at lowest TTL levels around the level of zero radiative heating in ERA-5 (about 350K)... This is important since there is no such level in ERA-I. But maybe I did not understand correctly (see SC27 below) in such case the text should be clarified.*
The text here refers to the general location of the level of zero radiative heating, not to a specific ERA5 level. We slightly modified the text to "in the lowest TTL around the level of zero radiative heating" to avoid mentioning specific TTL levels, and hope this is clearer now.

SC14. *Line 175: for clarity I suggest to insert here a preview of the Discussion, inserting few words e.g. This much weaker upwelling in the TTL and tropical lower stratosphere causes stronger restrictions on large-scale advective upward transport in ERA5 and appears to correct an overestimation in ERA-I (see section 6).*
Done.

SC15. *Lines 178-179: The upward velocities in ERA5 in that region are more consistent with the residual circulation vertical velocity (see next paragraph and Fig. 2). This transition does not work see next paragraph should be avoided. I*

suggest to move that sentence to the end of the next paragraph.
Wording has been modified.

SC16. *Lines 188 and 189: upwelling and downwelling are stronger but not strongest and tropical upwelling is stronger in DJF not in boreal winter (see SC12).*
Changed. However, we kept the wording "boreal winter" (see reply to SC12).

SC17. *Lines 196-197: up to 30-40%, see Fig. 1: normalized differences can not be seen on Fig.1 Above about 20 km...: what is the corresponding theta? See MC5. A proper comparison would actually require a figure that overlays the two vertical profiles of tropical dθ/dt as function of θ with the two vertical profiles of tropical $\overline{w}^*$ as a function of p.*
As $\overline{w}^*$ is the vertical velocity in log-pressure coordinates, while dθ/dt is the vertical velocity in isentropic coordinates, we think it is better to show each variable in the respective coordinate system. However, we added difference plots to all cases in Figs. 1 and 2 (as also suggested by Reviewer 1) to ease comparison and evaluation of the differences.

SC18. *Figure 3c and 3d are difficult to read due to lack of contrast between the blue colors that are also obscured by the black contour lines. Consider removing these black color lines (pressure levels and zonal wind contours are well sufficient) and/or changing the color map.*
We agree that the contrast in Fig. 3 is not optimal. However, we think it is better to keep the black contour lines of climatological mean age to ease evaluation of the relative differences. Also, we prefer to have a bipolar blue–red color map for difference plots, although the differences in that case are all negative.

SC19. *Line 223: the differences are not so clear since closer inspection is required. In the tropics the differences are definitely not clearly visible and would require actual lineplots of the spectra (which could be worth adding; see MC2).*
Although probably not optimal, we think the clarity of the differences is still good. As explained in the reply to MC2 we don't want to include more figures to have the paper not too lengthy. Hence, we just modified the wording here slightly, saying now "Closer inspection reveals differences...".

SC20. *Line 226: the words against exchange with middle latitudes are superfluous*
Changed accordingly.

SC21. *Line 237: ...faster transport of young air towards the pole in ERAInterim than in ERA5. This is not true everywhere: the northernmost latitudes in Fig. 5c show older modal age in ERA-I than in ERA-5.*
This statement concerned poleward transport in the summer hemisphere, as said at the beginning of the sentence. To make this clearer, we added a remark on the DJF case where poleward transport is faster in ERA–Interim in the SH (Fig. 5c). We hope this is clearer now.

SC22. *Lines 244-252: the negative age trend with ERA-5 is significant in (nearly) the whole stratosphere for the period 1989-2018. Similarly, the trends found with ERA-I for 1989-2018 are either negative either positive but significant nearly everywhere. These significances should be highlighted. Line 252: In the lowest tropical and sub-tropical stratosphere ERA5 shows significantly increasing age, although non-significant changes in some regions, compared to decreasing age or insignificant trends in ERAInterim in this region.*
Changed accordingly.

SC23. *Lines 265-271: I find this paragraph quite confusing. Here is a suggestion for a clarified version (assuming I understood correctly): The clearest difference to ERAInterim regarding structural age spectrum changes emerges at middle and high latitudes at upper levels (here 600K, Fig. 7b and d). ERA5, on the one hand, shows a shift of the spectrum to younger ages, although not as clear as in the tropics and in the SH. ; ERA Interim, on the other hand, shows a decrease in the fraction of air younger than about 4 years and an increase of the fraction of older air. This increasing fraction of air older than about 4 years in ERA Interim indicates that ERA-5 has a strengthening in the deep branch of the residual circulation. The different spectrum changes in ERA5 and ERAInterim cause the opposite mean age changes in the two reanalyses (Fig. 6)., and are related to different trends in the deep BDC branch (see next paragraph). The end of this paragraph aims to introduce the follwing one: this transition should be re-worded (see also MC6).*
We tried to further clarify this text, taking into account these comments and also a comment from Reviewer 1.

SC24. *Lines 299-304: please re-write for clarity and elaborate on the interpration. Here is a suggestion: ...mean age appears to increase before about 1991 in both hemispheres and after about the year 2000 (except in the SH) in the NH and decreases in between. These steplike changes are evident in both reanalyses. In the beginning of the 1990s they and could be related to the Pinatubo eruption (i.e. true atmospheric variability) while in the end of the 1990s they could be related*

to changes in the observing system assimilated by the reanalyses. In particular... Chabrillat et al. (2018) discussed the obscuring impact of the observing system change that happened less than a decade after Pinatubo (their section 3.2) so this reference may be used again here.
The text has been modified accordingly, and the Chabrillat et al. reference added here.

SC25. *Figure 10a: It seems to me that these AoA use as source region the tropical 100 hPa levels (rather than the surface in all your other plots). Please check and (if correct) state this fact in the figure caption. What time period covered in the ClaMS simulations is used for this figure? Does it match the observational values taken from Waugh (2009)? What is the exact uncertainty range indicated by the error bars, i.e. do they show 1-σ (66% confidence level) or 2-σ (95% confidence level) on each side of the observation? Better explanations about this figure will allow improving the corresponding discussion and go a long way in addressing the general comment.*
See mainly our reply to the general comment. Regarding the additional specific points here: The CLaMS age shown in Fig. 10a is consistent with the other data shown in the paper, hence with respect to the surface. The time periods in observational age and model age are, indeed, not the same (see general comment reply). This is stated now explicitly, with a more detailed description of observational uncertainties, in Sect. 5.

SC26. *SC26. Section 5 needs to be substantively improved (see General Comments). Here are some questions and superficial suggestions:*
Lines 310-311: ...ERA5 mean age values are just at outside the upper margin of the uncertainty range of the in-situ SF_6 -based observations. This apparent overestimation of mean age in ERA5 may be even larger in reality because Leedham Elvidge et al. (2018) have recently shown that...
Lines 315-316: ..ERA5 age is at or above the upper margin of the observational uncertainty range before about 1997, while ERAInterim is at in the lower margin part of the range (Fig. 10b).
Line 317: ...the more gradual increase in ERAInterim mean age... : over what period?
Line 320: ...we note the trend values from a simple linear regression...: over what period?
Line 328 and caption of Fig.11: ...(for a detailed measurement data description, see Laube et al., 2020). What tracer was used to derive this observational AoA? This should be stated in the text, along with an estimate of the associated uncertainty and also the uncertainty of the CFC-11 observations. It would be even better to show these uncertainties graphically in Fig. 11 if possible).
We modified and rewrote substantial parts of Sect. 5 as suggested and exchanged the correlation figure with a figure showing the difference between model and observation age (new Fig. 11), as already explained in the reply to the general comments above.

SC27. *Line 347: ...the minimum in tropical upwelling around the level of zero radiative heating (around 350K) is much lower for ERA5 than for ERAInterim.... I do not understand this formulation: is there a level of zero radiative heating in ERA-I as well? Do you mean something else than the minimum value itself? This is related to SC13 above.*
See our reply to SC13 above.

SC28. *Lines 353-354: it would be good to remind the reader about the corresponding pressure ranges i.e. ...while in the tropical lower stratosphere (50-150hPa) the representation of tropical upwelling seems to beimproved in ERA5, it is unclear whether the very weak total diabatic heating rates in the lower TTL (150-300hPa) are realistic.*
Approximate pressure ranges have been added to the text, as suggested.

SC29. *Lines 355-360: this paragraph should be revised (see general comment). More specifically: Line 355: ...age of air in ERA5 is slightly high-biased... but according to Fig. 10a this bias is significant and still 1 year older, i.e. as large as the difference between MERRA-2 and ERA-I in Chabrillat et al. (2018) or Ploeger et al. (2019). Hence slightly seems rather subjective to me... Line 358: It should be noted that these differences are small... with respect to what? Line 359: ...when taking all uncertainties into account. This is a quite vague formulation, especially considering that the uncertainties were not sufficiently described (see SC25 and SC26).*
This paragraph has been modified substantially, taking into account the Reviewer's suggestions and the improved comparison to in-situ observation-based age of air (see also reply to the general comment above).

SC30. *Line 362: ...which was argued by Stiller et al. (2017) to agree qualitatively with the structural circulation change observed by MIPAS. These MIPAS observations of structural circulation changes were first reported by Stiller et al. (2012). The agreement between AoA trends in observations and in ERA-Interim was first reported by Mahieu et al. (2014) using observations of HCl.*
The sentence here refers to the agreement between ERA–Interim and MIPAS age trends, not to the MIPAS age trends themselves. Therefore, we think the given reference to Stiller et al. (2017) is appropriate. The MIPAS trends are introduced already in the abstract, with proper referencing to the earlier paper by Stiller et al. (2012).

SC31. *Line 369: The globally negative age of air trend in ERA5 over 19892018 agrees with results from climate model simulations, showing an accelerating BDC and decreasing age over multi- decadal time scales in response to increasing greenhouse gas concentrations. This agreement may very well be for different reasons than increasing GHG concentrations because in ERA-5 NH the decreasing age is entirely due to the decrease in the 1990s (1993-2003) i.e. a timescale much shorter than in the CCM simulations (and probably related to Pinatubo eruption). See also MC1 and SC24 above.*
We agree that the age decrease in ERA5 is likely due to the age decrease in the mid-nineties. We discuss this aspect in the following paragraphs. We tried to further clarify the wording here and at other relevant places in the manuscript. (See also our replies to MC1 and SC24).

SC32. *Line 395: ...also before 1979 (as available from an extended ERA5 data product to be released soon). We can expect this backward extension to bring its own artifacts as the BDC will be much less constrained by satellite observations, with results more akin to those by climate models. In such a case the differences between CCM and ERA5 would most probably be related to shortcomings in the underlying model of ERA5 (i.e. IFS is an NWP model and not yet a climate model).*
This is a very valid remark, and we agree with this view. But still it will be very interesting to investigate the extended time period before 1979 in ERA5. Hence, we keep the formulation in the manuscript as is.

SC33. *Line 404: ...raises the question whether the remaining steplike change could be related to an incomplete bias correction in ERA5. Or maybe to a bias correction that started too late? A cursory look at the ECMWF report on ERA5.1 (Simmons et al., 2020) would help in this part of the discussion.*
We agree, and the suggested subsentence has been added.

SC34. *Line 421: ...and in the TTL ... According to your own discussion, it is not clear that the upwelling changes in the TTL are a correction.*
Thanks for pointing this inconsistency in our formulation out! We meant “upper TTL” here, and changed the text accordingly.

SC35. *Line 427: ...largely related to a steplike change around the year 2000. See above: your figures rather show two steplinke changes, one around 1993 and the other one around 2000.*
Again, thanks for pointing to that! “year 2000” here was just wrong. We meant “in the mid-nineties”, and changed the text accordingly.

SC36. *Line 435: what is the availability of the observational data shown in Fig. 10 and 11?*
There is no new observational data set compiled for this paper. All observational data shown here has already been published elsewhere, with related data availability statements (e.g., the data in Fig. 10a was compiled by Waugh and Hall (2002), the data in Fig. 10b published by Engel et al. (2017), and the data in Fig. 11 by Laube et al. (2020)).

Typos, wording, etc.:

L4: *Line 4: ERA5-based results are compared to those using the preceding ERAInterim reanalysis.*
Changed to “based on the preceding...”

L34: *Line 34: Waugh and Hall (2002) is a review paper on this diagnostic, hence the e.g. is not necessary.*
Changed.

L101: *Line 101: ...a pulse period of 2 months.*
We think “frequency” is more appropriate here, as this text refers to the frequency that a pulse occurs and not to the period of one specific pulse (which would be 10 years).

L153: *Line 153: For instance, the forecast data starting at 6UTC and on the 5th hour forecast step.... Same for line 161.*
As the text refers to “forecast data” as a data set provided by the ECMWF at a specific time and not to the “forecast” itself, we think the formulation is more appropriate as is.

L157: *Line 157: Here the hourly ERA5 data is not used to drive model transport but data sub- sampled in time is used instead, hence the temperature tendencies...*
Changed accordingly.

L178: *Line 178: where ERA5 shows upward velocities whereas they are downward in ERA Interim.*
Changed as suggested.

L205: *Line 205: ...apparent in both reanalyses.*
Corrected.

L207: *Line 207: ...critically...*
Corrected.

L220: *Line 220: abbreviation NH not yet defined.*
NH is defined now in the introduction.

L231: *Line 231: clear detailed differences occur in the details of the spectrum shape*
Having "details" twice sounds somewhat complicated to us, hence we keep the formulation as is.

L246: *Line 246: However above about 500 K and in particular in the NH, the signs of the trends...*
As the trends are only opposite in the NH we think the existing formulation is more appropriate.

L286: *Line 286: ...shows increasing RCTTs, clearest with strongest positive trends in the NH.*
As the text should say that "increasing RCTTs are clearest in the NH" we think it is more appropriate as is.

L290: *Line 290: ...(compare with Fig.6).*
Changed as suggested.

L293: *Line 293: ...the variability periodicity is similar at all locations... or maybe the timing of the variability is similar at alo locations*
Here, we only want to do a qualitative comparison (sentence starts already with "From a qualitative point of view..."), and we don not want to have the formulation too specific to suggest more.

L309: *Line 309: The latitudinal distribution in ERA-Interim (Fig. 10a) agrees well with...*
Changed as suggested.

L372: *Line 372: ... this accelaration of the residual circulation...*
Changed.

The stratospheric Brewer–Dobson circulation inferred from age of air in the ERA5 reanalysis

Felix Ploeger[1,2], Mohamadou Diallo[1], Edward Charlesworth[1], Paul Konopka[1], Bernard Legras[3], Johannes C. Laube[1], Jens-Uwe Grooß[1], Gebhard Günther[1], Andreas Engel[4], and Martin Riese[1]

[1]Institute for Energy and Climate Research: Stratosphere (IEK–7), Forschungszentrum Jülich, Jülich, Germany.
[2]Institute for Atmospheric and Environmental Research, University of Wuppertal, Wuppertal, Germany.
[3]Laboratoire de Météorologie Dynamique, UMR8539, IPSL, UPMC/ENS/CNRS/Ecole Polytechnique, Paris, France.
[4]Institute for Atmospheric and Environmental Sciences, Goethe-University Frankfurt, Frankfurt, Germany.

Correspondence: Felix Ploeger (f.ploeger@fz-juelich.de)

Abstract. This paper investigates the global stratospheric Brewer-Dobson circulation (BDC) in the ERA5 meteorological reanalysis from the European Centre for Medium-Range Weather Forecasts (ECMWF). The analysis is based on simulations of stratospheric mean age of air, including the full age spectrum, with the Lagrangian transport model CLaMS, driven by reanalysis winds and total diabatic heating rates~~from the reanalysis~~. ERA5-based results are compared to ~~those of~~ results based on the preceding ERA–Interim reanalysis. Our results show a significantly slower BDC for ERA5 than for ERA–Interim, manifesting in weaker diabatic heating rates and larger age of air. In the tropical lower stratosphere, heating rates are 30–40% weaker in ERA5, likely correcting a ~~known~~ bias in ERA–Interim. ~~Above~~At 20km and in the NH stratosphere, ERA5 age ~~of air appears slightly high-biased and the BDC slightly slow compared to tracer observations~~values are at the upper margin of the uncertainty range from tracer observations, indicating a comparatively slow BDC. The age trend in ERA5 over 1989–2018 is negative throughout the stratosphere, as climate models predict in response to global warming. However, the age decrease is not linear ~~over the period but exhibits steplikechanges which could be caused by muti-annual~~ but steplike, potentially caused by multi-annual variability or changes in the ~~assimilation system. Over the~~ observations included in the assimilation. During 2002–2012~~period~~, ERA5 age shows a similar hemispheric dipole trend pattern as ERA–Interim, with age increasing in the NH and decreasing in the SH. Shifts in the age spectrum peak and residual circulation transit times indicate that reanalysis differences in age are likely caused by differences in the residual circulation. In particular, the shallow BDC branch accelerates ~~similarly~~ in both reanalyses while the deep branch accelerates in ERA5 and decelerates in ERA–Interim.

1 Introduction

The Brewer-Dobson circulation (BDC) is the global transport circulation in the stratosphere, controlling the transport of chemical species and aerosol (e.g., Holton et al., 1995; Butchart, 2014). Changes in the BDC induce changes in radiatively active trace gas species and hence may cause radiative effects on climate. Therefore, BDC changes need to be reliably represented in atmospheric models.

The BDC is characterized by upwelling motion in the tropics, poleward transport in the stratosphere and downwelling above middle and high latitudes. In addition, a mesospheric circulation branch transports air masses from the summer to the winter pole. As pointed out by Haynes et al. (1991), ~~this circulation~~ the BDC is mechanically driven by atmospheric waves propagating upwards from the troposphere and breaking at upper levels in the stratosphere where they deposit their momentum and cause the driving force. From a conceptual point of view, the BDC can be divided into a residual mean mass circulation and additional two-way eddy mixing (e.g., Neu and Plumb, 1999; Garny et al., 2014), which are both related to the breaking of atmospheric waves. The residual circulation and eddy mixing both affect trace gas distributions in a complex manner (e.g., Minganti et al., 2020). The climatological structure of the BDC shows two main circulation branches: a shallow branch at lower levels (below about 20 km) which causes rapid transport to high latitudes (transport time scales of months), and a deep branch above with much longer transport time scales of a few years (e.g., Plumb, 2002; Birner and Bönisch, 2011; Lin and Fu, 2013).

Diagnosing the BDC and estimating its strength is a challenging task due to the fact that the BDC is a zonal mean circulation and that the mean vertical velocities are very slow (less than 1 mm/s). In models, these slow velocities can be computed (e.g., within the Transformed Eulerian Mean (TEM) framework, Andrews et al., 1987), but are likely affected by model numerics. For observations, the circulation strength needs to be deduced from trace gas measurements. A common diagnostic for the speed of the BDC is the stratospheric age of air ~~(e.g., Waugh and Hall, 2002)~~(Waugh and Hall, 2002). Due to atmospheric mixing processes, a given air parcel in the stratosphere is characterized by a multitude of different transit times through the stratosphere, defining the age spectrum (Hall and Plumb, 1994). The first moment of the age spectrum defines the mean age of air. Due to its definition of being an average transit time, mean age may give ambiguous results, while the age spectrum is able to resolve the information ~~of different processes (e.g., Waugh and Hall, 2002)~~on different processes (Waugh and Hall, 2002).

Despite its crucial effects on atmospheric composition and climate no common understanding of long-term changes of the BDC with increasing greenhouse gas levels has been reached yet. On the one hand, climate models show a robust strengthening and acceleration of the BDC with climate change (e.g., Butchart et al., 2010), manifesting in an increase in tropical upwelling and a decrease in global mean age of air. On the other hand, atmospheric trace gas measurements from balloon soundings at ~~NH~~ Northern hemisphere (NH) mid latitudes show a non-significant long-term BDC trend over the last decades (Engel et al., 2009, 2017; Fritsch et al., 2020). Also satellite measurement from the Michelson Interferometer for Passive Atmospheric Sounding (MIPAS) show no globally homogeneous mean age change over the 2002–2012 period but a more detailed pattern with increasing age in the ~~Northern hemisphere (NH)~~ NH and decreasing age in the Southern hemisphere (SH) (Stiller et al., 2012; Haenel et al., 2015).

Coming along with improvements in model physics and data assimilation systems, meteorological reanalyses have been used more intensively for trend investigations during recent years. With transport driven by ECMWF ERA–Interim reanalysis modelling studies have shown a weak increase of mean age in the NH middle stratosphere, qualitatively consistent with balloon observations (e.g., Diallo et al., 2012; Monge-Sanz et al., 2012). However, more recent efforts combining different newest generation reanalysis data sets have shown a large dependency of BDC trend estimates on the reanalysis used, for both residual circulation (Abalos et al., 2015; Miyazaki et al., 2016) and age of air diagnostics (Chabrillat et al., 2018; Ploeger et al., 2019). ~~Hence, while inter-annual BDC variability seems to be well represented in reanalyses, regarding decadal changes and~~

~~trends~~ In particular concerning decadal age of air and BDC changes no consensus has been reached amongst reanalyses, including ERA–Interim reanalysis from the European Centre for Medium-Range Weather Forecasts (Dee et al., 2011), JRA–55 from the Japanese Meteorological Agency (Kobayashi et al., 2015), and MERRA–2 from the National Aeronautics and Space Administration (Gelaro et al., 2017).

Very recently, the ECMWF has released its newest generation reanalysis product ERA5 (Hersbach et al., 2020). Compared to its predecessor ERA–Interim, ERA5 is based on an improved forecast model version and improved data assimilation system (see Sect. 2.2 for further details). Case studies on stratospheric and tropospheric transport indicate improvements in the representation of physical processes, like convection, in ERA5 (e.g., Li et al., 2020). Recently, Diallo et al. (2020) have analyzed the ERA5 residual mean mass circulation of the BDC, its variability and trend, based on Transformed Eulerian mean (TEM) calculations. The present paper can be viewed complementary as it investigates the representation of the BDC in ERA5 in terms of stratospheric age of air from transport model simulations, and compares results to the previous ERA–Interim reanalysis. For that reason, we carry out simulations of stratospheric age of air with the Lagrangian CLaMS model (Chemical Lagrangian Model of the Stratosphere) over the period 1979–2018 driven with either ERA5 or ERA–Interim reanalysis meteorology. Simulation of the stratospheric age spectrum with CLaMS allows pinpointing differences between the reanalyses to processes. The main research questions are: (i) How strong and fast is BDC transport in ERA5 compared to ERA–Interim? (ii) How has the BDC (and age of air) ~~been changing~~ changed over recent decades? (iii) How good is the agreement with age of air derived from trace gas observations? The analysis presented here contributes to the Processes And their Role in Climate (SPARC) Reanalysis Intercomparison Project S-RIP (Fujiwara et al., 2017) and can be regarded as a follow-up of the analyses presented by Chabrillat et al. (2018) and Ploeger et al. (2019), where the BDC in ERA–Interim, JRA–55 and MERRA–2 reanalysis was compared in terms of age of air~~, and~~. Here, we discuss the ERA5 results within the context of the other reanalyses. For better comparability, we also present ERA–Interim results from Ploeger et al. (2019)~~here~~, although for an extended period, and juxtapose them with the new ERA5 results.

In a first step in Sect. 2 the CLaMS model and age spectrum calculation ~~is~~ are described, as well as ERA5 reanalysis data. A particular focus is laid on the ERA5 diabatic heating rate which is used to drive CLaMS model transport. Thereafter, Sect. 3 presents the results related to the climatological structure of the BDC, showing that ERA5 has a substantially slower BDC than ERA–Interim. Section 4 presents BDC and age of air trends, showing a globally negative long-term trend for ERA5 and a stronger variability compared to ERA–Interim. A comparison to age of air observations is presented in Sect. 5. The results are placed into context of previous studies in the discussion in Sect. 6, and final conclusions are summarized in Sect. 7.

2 Data and method

In this study, the BDC is investigated based on age of air calculated with the CLaMS model driven with ERA5 and ERA–Interim reanalysis data. In the following, Sect. 2.1 describes the CLaMS model and age of air calculation while Sect. 2.2 briefly describes the ERA5 reanalysis with focus on the used variables.

2.1 Age of air simulations with the Chemical Lagrangian Model of the Stratosphere (CLaMS)

The CLaMS model is a Lagrangian chemistry transport model, with the transport scheme based on the calculation of three-dimensional air parcel trajectories (which represent the model grid points) and a parameterization of small-scale atmospheric mixing (McKenna et al., 2002; Konopka et al., 2004). This mixing parameterization is controlled by the shear in the large-scale flow (via a critical Lyapunov exponent), such that in regions of large flow deformations strong mixing occurs. The forward trajectory calculation is driven with offline meteorological data. In this paper, we will use ERA5 and ERA–Interim reanalysis data which are further described in Sect. 2.2.

In the vertical direction CLaMS uses an isentropic vertical coordinate which makes the model particularly well-suited for the stratosphere, where diabatic transport is generally weaker than adiabatic transport (e.g., McKenna et al., 2002). Strictly speaking, the vertical coordinate in CLaMS is a hybrid potential temperature which is orography-following at the surface and transforming smoothly into potential temperature ~~above~~ θ above, such that it equals θ ~~in~~ above the $\sigma = 0.3$ surface (with $\sigma = p/p_{\mathrm{surf}}$), hence throughout the stratosphere (e.g., Mahowald et al., 2002; Pommrich et al., 2014). The cross-isentropic vertical velocity (also termed diabatic vertical velocity, in the following) is calculated from the reanalysis total diabatic heating rate (see Sect. 2.2 for further details).

A calculation of the fully time-dependent stratospheric age of air spectra has been implemented in CLaMS, based on multiple tracer pulses, as described by Ploeger et al. (2019), and references therein. The age spectrum $G(r,t,\tau)$ at a point r in the stratosphere and time t is the distribution of transit times τ from the surface (or from the tropopause in some studies) to r. For the age spectrum calculation in CLaMS, chemically inert model tracers are pulsed in the orography-following lowest model layer (approximately the boundary layer) in the tropics (30°S–30°N) with unit mixing ratio, a pulse duration of 1 month and a pulse frequency of 2 months. The value of the age spectrum at transit time τ_i is then related to the mixing ratio χ_i of the tracer pulsed at $t - \tau_i$ and sampled at r (e.g., Li et al., 2012)

$$G(r,t,\tau_i) = \chi_i \; . \qquad (1)$$

Therefore, the use of 60 pulse tracers in the model with pulse frequency 2 months allows calculation of the age spectrum over 10 years ~~along~~ transit time (e.g., Ploeger et al., 2019). Mean age Γ is the average stratospheric transit time and is defined as the first moment of the age spectrum

$$\Gamma(r,t) = \int_0^\infty \mathrm{d}\tau \, \tau \, G(r,t,\tau) \; . \qquad (2)$$

The two model simulations driven with either ERA5 or ERA–Interim cover the period 1979–2018. Preceding 10 year spin-up simulations have been carried out by repeating the meteorology of 1979. To eliminate influence of this spin-up on the age spectra we ~~analyze~~ focus on the period 1989–2018, ~~in the following~~for most parts of the paper, when all memory of the spin-up in the 10 year long age spectra is lost. As the model age spectrum is truncated at 10 years the respective mean age will be low biased if no correction for the spectrum tail is taken into account. Therefore, throughout this paper we consider mean age calculated from an additional “clock-tracer” in CLaMS, a chemically inert tracer with linearly increasing mixing ratios at the surface (e.g., Hall and Plumb, 1994). This clock-tracer mean age had experienced a longer spin-up (minimum 20 years, at the beginning of the considered period in 1989), and is therefore larger compared to the spectrum-based mean age.

In addition to age of air, we also consider CFC–11 from CLaMS simulations in Sect. 5. The simulations include a simplified chemistry scheme (Pommrich et al., 2014) such that CFC–11 is affected only by photolytical loss. Both mean age and CFC–11 simulated with CLaMS agree well with stratospheric observations (e.g., Ploeger et al., 2019; Laube et al., 2020). Note that compared to Ploeger et al. (2019) small quantitative differences can occur due to different periods considered, and also due to the use of different mean age calculation methods (clock-tracer versus spectrum-based), and also due to different periods considered(clock-tracer versus spectrum-based, for a quantification of these differences see Ploeger and Birner, 2016, Figs. 4 and A1) . Another difference to the simulations by Ploeger et al. (2019) concerns the cross-isentropic vertical velocities. Ploeger et al. (2019) added a constant correction term to the vertical velocity to correct for missing balance in the annual mean cross-isentropic mass flux on a given θ-level, as suggested by Rosenlof (1995) and implemented in CLaMS by Konopka et al. (2010). Here, we do not include this mass correction and use the "raw" reanalysis heating rate to simplify interpretation and reproducibility with other studies. For most of the results including this annual mean mass balance causes no significant change. Only for mean age trends after about 2002 it causes a clearer age decrease in the SH (see Sect. 4).

2.2 ERA5 reanalysis

The newest generation ERA5 reanalysis from the European Centre for Medium-Range Weather Forecasts (ECMWF) is the successor of the previous ERA–Interim reanalysis (Dee et al., 2011). ERA5 is now available from 1979–2020 with production lagging real time by about 2 months. For the production of ERA5, 4D–Var data assimilation of the ECMWF Integrated Forecast System (in cycle CY41R2) was used (Hersbach et al., 2020). The horizontal resolution is about 30 km (T639). In the vertical, the pressure range from the surface to 0.01 hPa is covered with 137 hybrid levels. The output frequency for ERA5 data is hourly. Due to a cold bias in the lower stratosphere, the reanalysis data has been replaced for the period 2000–2006 with the updated data named ERA5.1 (Simmons et al., 2020). For the present paper, we carried out CLaMS simulations driven with both the previous (termed ERA5.0 in the following) and the corrected ERA5.1 data (for simplicity, termed ERA5 in this paper), and discuss effects of the bias correction on the stratospheric BDC (Sect. 6). Further details on ERA5 can be found in Hersbach et al. (2020).

For better comparability between the ERA5 and ERA–Interim driven model simulations as well as for practicability reasons (storage and memory space) we use 6-hourly (0, 6, 12, 18 UTC) ERA5 data with truncated 1×1 degree horizontal resolution, downscaled using direct transformation from T1279 to 1×1 degree with automatic truncation to T213 as provided by the ECMWF MARS processing system. However, we maintain the full vertical resolution, as the necessary meteorological data is interpolated from the reanalysis fields on native ECMWF model levels onto the Lagrangian CLaMS air parcels. Hence, the ERA5 data to drive the CLaMS model in this study has 137 hybrid ECMWF model levels, for ERA–Interim 60 levels.

Of particular importance for the CLaMS model calculations is the reanalysis temperature tendency variable (diabatic heating rate) which is used for deducing diabatic vertical velocity(diabatic heating rates). Both ERA5 and ERA–Interim provide 5 temperature tendencies: The mean temperature tendencies due to short-wave and long-wave radiation for both clear-sky and all-sky conditions, as well as the mean temperature tendency due to ~~parametrisations~~all parametrisations (including the mentioned radiative contributions, latent heat release, turbulent and sensitive heating). From the temperature tendency due to parametrisations (the total diabatic heating rate Q_{tot}) the cross-isentropic vertical velocity $\mathrm{d}\theta/\mathrm{d}t$ for driving CLaMS transport is calculated as

$$\frac{\mathrm{d}\theta}{\mathrm{d}t} = \frac{\theta}{c_p T} Q_{\text{tot}} \,, \tag{3}$$

with T temperature, θ potential temperature, and c_p the specific heat capacity at constant pressure. The calculation of cross-isentropic vertical velocity for ERA–Interim was described by Ploeger et al. (2010). In the following, we illustrate the similar (but not identical) procedure for ERA5.

Temperature tendencies are only available from the ERA5 forecast data, which is stored twice per day (6, 18 UTC) with forecast steps ranging between 1 and 18 hours (1 hour increments). These temperature tendencies have to be interpreted differently compared to ERA–Interim, as they are “mean rates”, representative for the interval between the actual time and the previous post processing time. For instance, the forecast data at 6 UTC and 5 hour forecast step is the mean tendency between 10 and 11 UTC. Temperature tendencies are provided in K/s (Kelvin per second). The CLaMS pre-processor assigns the forecast variables to the reanalysis data set at the later time (here 11 UTC). This induces a time uncertainty of 0.5 hours, which is negligible for the purpose of this paper.

~~In cases where not~~ Here we did not use the hourly ERA5 data ~~is used~~ to drive model transport but data sub-sampled in time is used instead. Therefore, the temperature tendencies have to be averaged appropriately, as they represent accumulations since the previous post processing time and not since the last forecast date. Otherwise, sampling errors will occur. Hence, for the present case of using only 0, 6, 12, 18 UTC data we average all tendency data sets within 6 hour windows around each date. For instance, the mean tendency averaged over 10-15 UTC (from forecast data at 6 UTC with 4-9 hour steps, see above) is assigned to the reanalysis data at 12 UTC.

3 Climatological view on the stratospheric circulation

As described in Sect. 2, CLaMS uses diabatic heating rates for driving vertical transport in the model. The climatological cross-isentropic (or diabatic) vertical velocity $\mathrm{d}\theta/\mathrm{d}t$ calculated from the diabatic heating rate for winter and summer seasons from ERA5 and ERA–Interim~~is~~, and the respective differences, are shown in Fig. 1 ~~a–d~~a–f. Overall, both reanalyses show very similar distributions and seasonality for $\mathrm{d}\theta/\mathrm{d}t$. ~~Cross-isentropic~~ Diabatic tropical upwelling maximizes in boreal winter (December–February, DJF), somewhat shifted into the summer subtropics, and the extratropical downwelling maximizes in the respective winter hemisphere. Further, heating rates show a double-peak structure above the tropical tropopause with a minimum above the equator. However, ~~clear quantitative~~ quantitatively also clear differences occur between the two reanalyses~~.~~ ~~The~~, showing larger diabatic velocities (heating rates) in the lower stratosphere (positive differences below about 600 K, Fig. 1 c, f) in ERA–Interim and smaller heating rates above. In particular, the zoomed view in Fig. 1 ~~e–g~~ g–i reveals that in the layer 400-430 K (30°N/S) ERA–Interim shows about 40% larger total diabatic heating rates than ERA5. Furthermore, ~~at lowest~~

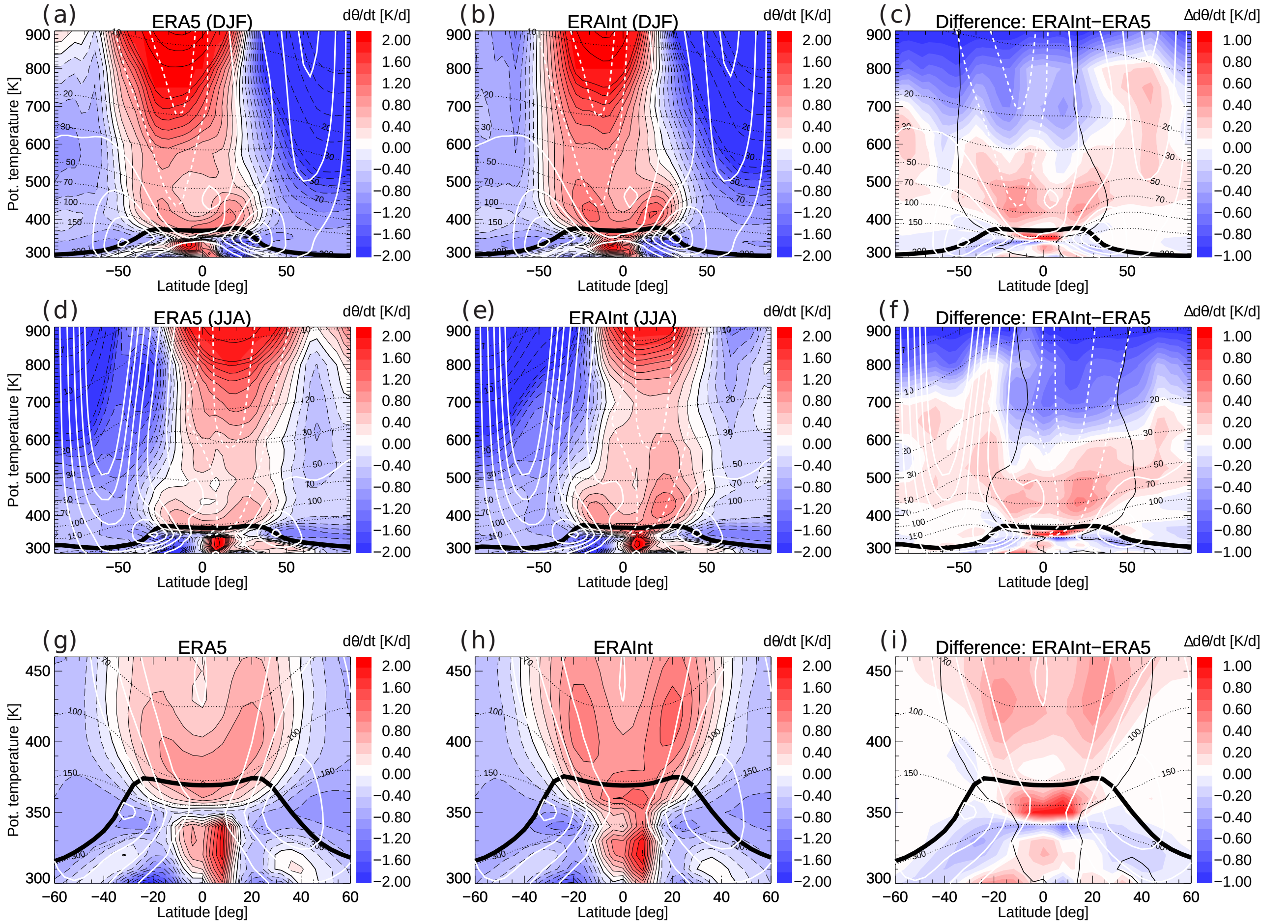

Figure 1. ~~Total diabatic heating rate~~ Diabatic vertical velocity $d\theta/dt$ climatology (1979–2018), calculated from ~~(a) ERA5 during~~ the total diabatic heating rate, for boreal winter (December–February, DJF) ~~and~~ from (~~b~~a) ~~during summer~~ ERA5, (~~June–August~~b) ERA–Interim, ~~JJA~~and (c) the difference ERA–Interim minus ERA5. (~~c, d~~d–f) Same but ~~from ERA–Interim.~~ for boreal summer (~~e~~June–August, ~~f~~JJA). (g–i) Zoomed view into the tropical lower stratosphere on annual mean heating rates~~, and (g)~~. Note the ~~respective difference ERA–Interim minus ERA5 (thin black countour in~~ different color scale for the difference ~~plot shows the zero contour from ERA–Interim)~~plots. Heating rate contours are highlighted in black (dashed for negative values). The thin black countour in the difference plot shows the zero contour from ERA–Interim. White contours show zonal wind (in ±10 m/s steps; easterly wind dashed), thin dashed black lines pressure levels, the thick black line the (WMO lapse rate) tropopause.

~~TTL levels~~ in the lowest TTL around the level of zero radiative heating (about 350 K) total diabatic heating rates are much weaker in ERA5 than ERA–Interim, with even no continuous upwelling in the annual mean in a shallow layer around 350 K (Fig. 1~~g~~i). It should however be noted, that seasonal ERA5 heating rate averages show very weak zonal mean upwelling from the troposphere into the stratosphere in small latitude bands, which vanishes in the annual mean due to seasonal shifts. This

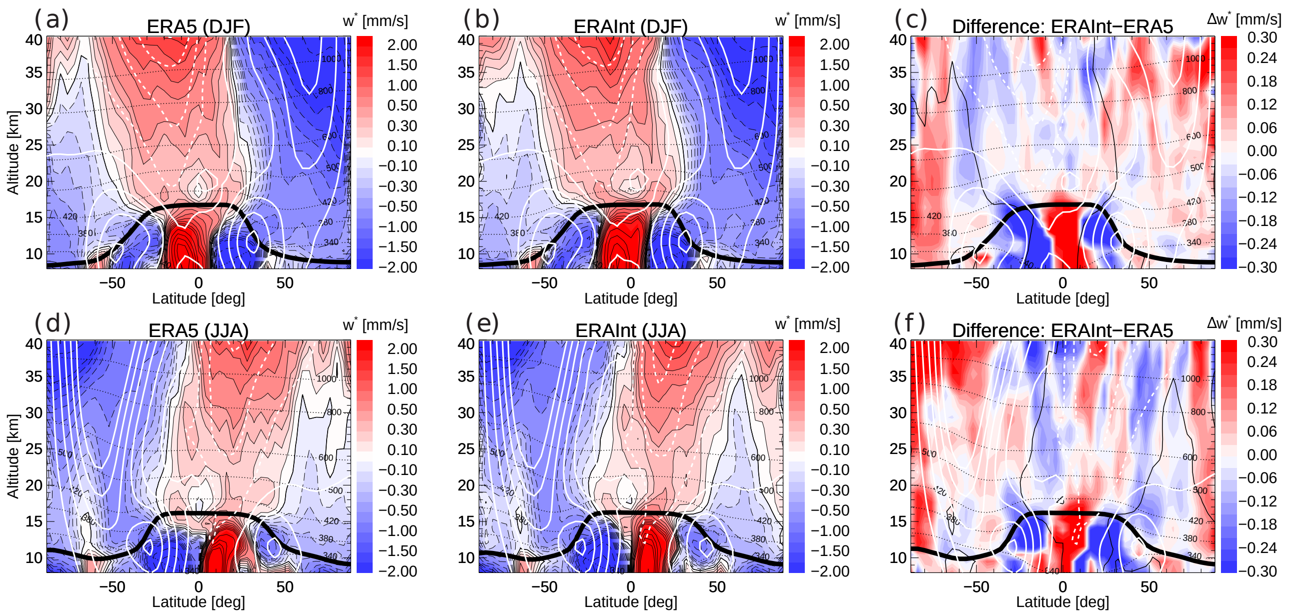

Figure 2. Residual circulation vertical velocity $\overline{w}^*$ climatology (1979–2018) ~~from (a) ERA5 during~~ for boreal winter (December–February, DJF) ~~and~~ from (~~b~~a) ~~during summer~~ ERA5, (~~June–August~~b) ERA–Interim, ~~JJA~~and (c) the difference ERA–Interim minus ERA5. (~~c, d~~d–f) Same but ~~from ERA–Interim~~for boreal summer (June–August, JJA). Note the different color scale for the difference plots. Circulation contours are highlighted in black (dashed for negative values). White contours show zonal wind (in ±10 m/s steps; easterly wind dashed), thin dashed black lines potential temperature levels, the thick black line the (WMO lapse rate) tropopause. The y-axis is log-pressure altitude.

much weaker upwelling in the TTL and tropical lower stratosphere causes stronger restrictions on large-scale advective upward transport in ERA5 and appears to correct an overestimation in ERA–Interim (see Sect. 6. The heating rate difference below the tropopause will also affect the simulations of mean age, which is defined with respect to the surface in this study. Another difference between the two reanalyses concerns heating rates in the summertime stratosphere above about ~~800~~700 K (about 20 hPa), where ERA5 shows upward velocities whereas ERA–Interim shows downward velocities. The upward velocities in ERA5 in that region are more consistent with the residual circulation vertical velocity (~~see next paragraph and~~ Fig. 2), which is further discussed below.

Diallo et al. (2020) analyzed the ERA5 BDC based on the TEM residual circulation vertical velocity, a common measure for the strength of the BDC (e.g., Andrews et al., 1987, Eq. 3.5.1b),

$$\overline{w}^* = \overline{w} + \frac{1}{a\cos\phi}\,\partial_\phi\left(\cos\phi\,\frac{\overline{v'\theta'}}{\partial_z\overline{\theta}}\right)\,, \qquad (4)$$

where the overline denotes the zonal mean and primes fluctuations therefrom (due to eddies), w is the vertical velocity in log-pressure z coordinates, a is the Earth's radius, ϕ latitude, and v is the latitudinal wind component. Here, we briefly recapitulate a few findings from that paper for ease of comparison to the heating rate based results.

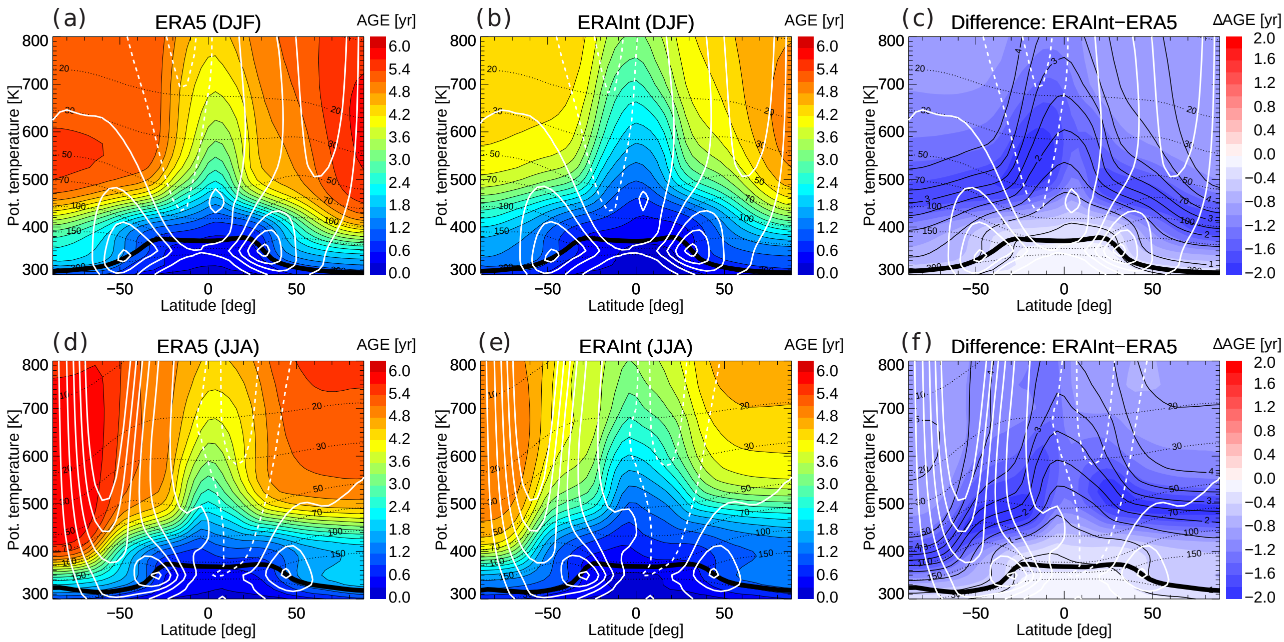

Figure 3. Mean age climatology (1989–2018) for boreal winter (December–February, DJF) from ERA5 (a), ERA–Interim (b), and the difference (c). (d, e, f) Same, but for boreal summer (June–August, JJA). White contours show zonal wind (in ± 10 m/s steps; easterly wind dashed), thin dashed black lines pressure levels, the thick black line the (WMO lapse rate) tropopause.

Figure 2 shows $\overline{w}^*$ calculated from ERA5 and ERA–Interim during boreal winter (December–February, DJF) and summer (June–August, JJA) and the respective reanalysis differences, for comparison with the diabatic ~~heating rates~~vertical velocity, calculated from the reanalysis diabatic heating rate. Overall, the $\overline{w}^*$ distributions and seasonal differences for both reanalyses are very similar. Also for $\overline{w}^*$, both reanalyses show ~~strongest~~ stronger tropical upwelling in boreal winter, somewhat shifted into the summer subtropics, and ~~strongest~~ stronger downwelling in the respective winter hemisphere. In particular in the winter hemisphere, contours of negative $\overline{w}^*$ representing downwelling are very close for both reanalyses. Also in the deep tropics close to the equator around the 18 km level (about 420 K potential temperature, 70 hPa pressure), a minimum in upwelling (even downwelling in JJA) occurs similarly in both data sets. Minor differences between ERA5 and ERA–Interim concern downward velocities in the summer hemisphere and a stronger upwelling in the tropical lower stratosphere in ERA–Interim. Diallo et al. (2020) showed in their Fig. 2 that tropical upwelling differences in $\overline{w}^*$ in the tropical lower stratosphere amount to about 40% at around 15 km and decrease above (zero difference at about 22 km). Hence, in the ~~tropical lower stratosphere~~ TTL the reanalysis differences in upwelling as diagnosed from $\overline{w}^*$ are qualitatively similar to those diagnosed from heating rates (up to 30-40%, see Fig. 1). Above about 20 km, however, upwelling from heating rates shows larger differences than upwelling from $\overline{w}^*$. Downwelling differences are larger in the summer than winter hemisphere, similar to the case of $\mathrm{d}\theta/\mathrm{d}t$.

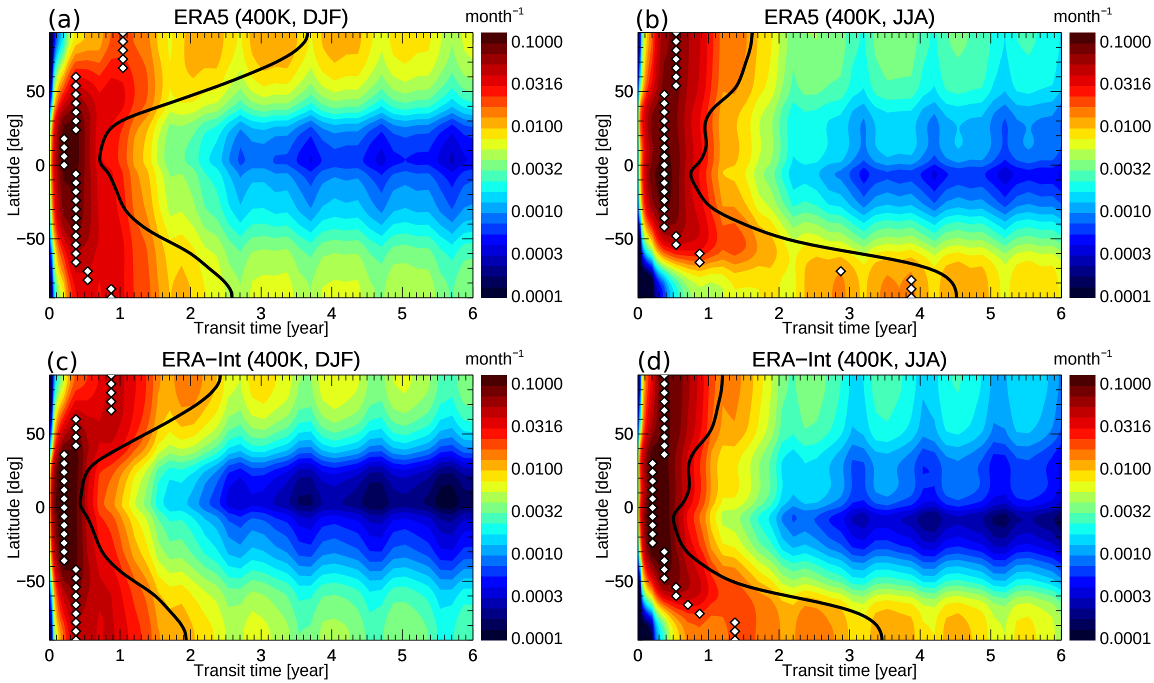

Figure 4. Age spectra at 400 K (1989–2018 climatology) from ERA5 for boreal winter (a) and summer (b). (c, d) Same, but for age spectra from ERA–Interim. Black contour shows mean age (calculated as first moment of spectra), white diamonds show modal age (peak of the spectrum).

The integrated effect of BDC transport in the two reanalyses is shown from climatological mean age of air for winter and summer in Fig. 3. The general characteristics of the stratospheric mean age distribution are evident for both reanalyses, with age increasing with both altitude and latitude, low age in the tropical upwelling region and high age in extratropical downwelling regions. Oldest air is ~~always~~ found in the winter hemisphere, even older in the SH during JJA compared to NH during DJF. The summertime lowest stratosphere (below about 450 K) is characterized by a “flushing” with young air (e.g., Hegglin and Shepherd, 2007; Bönisch et al., 2009), strongest in the NH during JJA. A particular feature in this region is an age inversion in the summertime NH with younger air (around 400 K) located above older air (around 350 K), which is also apparent in both ~~reanalysis~~reanalyses. This “eave structure” (i.e., younger air above older air) in the summertime lower stratosphere age distribution has been recently discussed by Charlesworth et al. (2020) and has been shown to depend ~~critially~~ critically on the numerics of the model transport scheme.

Clear quantitative differences between ERA5 and ERA–Interim age are evident in Fig. 3c and f, with significantly older air for ERA5. Largest differences of up to about 2 years (equivalent to about 50–75%) occur in the lower ~~stratospheric~~ stratosphere regions where the climatological age distribution (black contours) shows strongest gradients. These differences indicate a downward shift of the ~~regions~~ locations of strongest age gradients and stronger gradients in ERA5 compared to ERA–Interim.

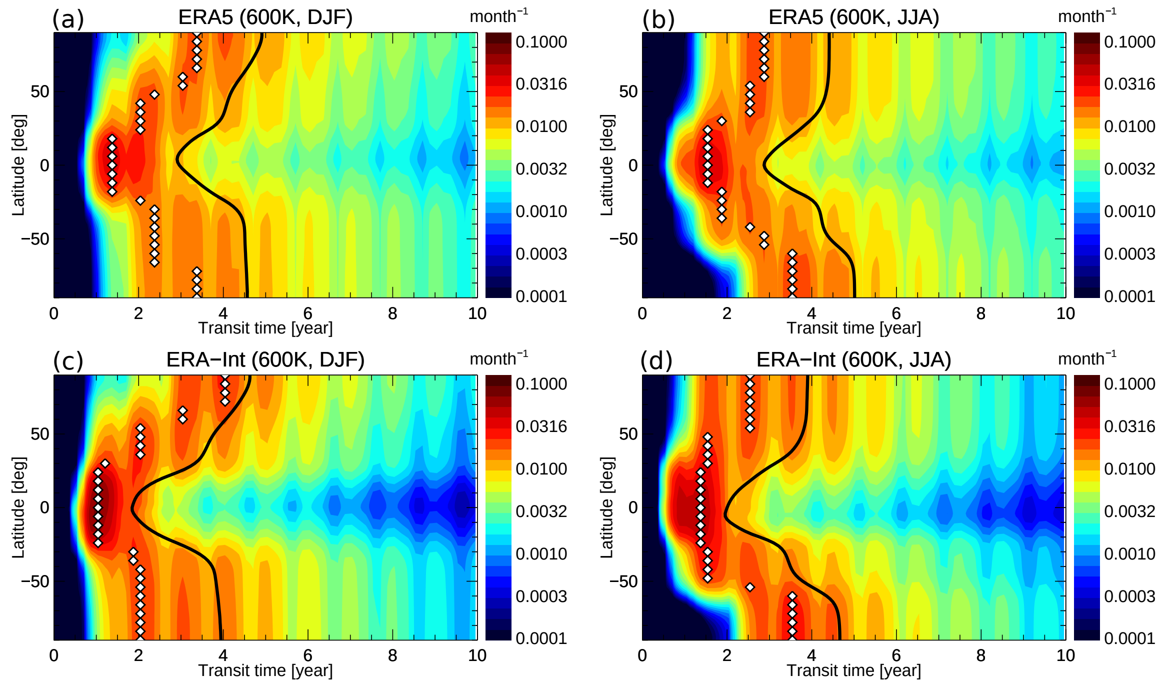

Figure 5. Same as Fig. 4 but at 600 K.

To gain deeper insight into transport processes and their differences in the two reanalyses, we consider stratospheric age spectra at 400 K and 600 K potential temperature levels, representative for the shallow and the deep BDC branch, respectively (see Fig. 2 for a relation between potential temperature and altitude levels). Figure 4 shows the CLaMS model age spectra at 400 K versus latitude for ERA5 and ERA–Interim for winter and summer. The spectra from both reanalyses show similar overall characteristics and seasonality, caused by known characteristics of BDC transport. The multi-modal spectrum shape, arising from the seasonality in upward transport into the stratosphere and in the strength of transport barriers, clearly emerges for both cases and appears strongest for middle latitude and high latitude spectra, consistent with previous studies (e.g., Reithmeier et al., 2007; Li et al., 2012). In the tropics, age spectra are narrower and with a younger peak in boreal winter, indicating faster upwelling during that season. Weaker latitudinal gradients in the summer hemisphere, especially in the NH during JJA, are a sign of stronger mixing in summer. The flushing of the summertime lower stratosphere with young air can be seen from the extent of the young air peak to high latitudes in the summer hemisphere (e.g., Fig. 4b, d).

Closer inspection reveals ~~also clear~~ differences between ERA5 and ERA–Interim age spectra. In the tropics, the main spectrum peak is broader and shifted to larger transit times for ERA5, related to slower tropical upwelling compared to ERA–Interim. At high latitudes this shift of ERA5 age spectra towards older transit times is even clearer, indicating slower transport along the BDC and a stronger confinement of polar regions ~~against exchange with middle latitudes~~ in ERA5. Clearest differences occur in the SH polar vortex during winter (JJA) where the modal age (transit time of the largest spectrum peak) for

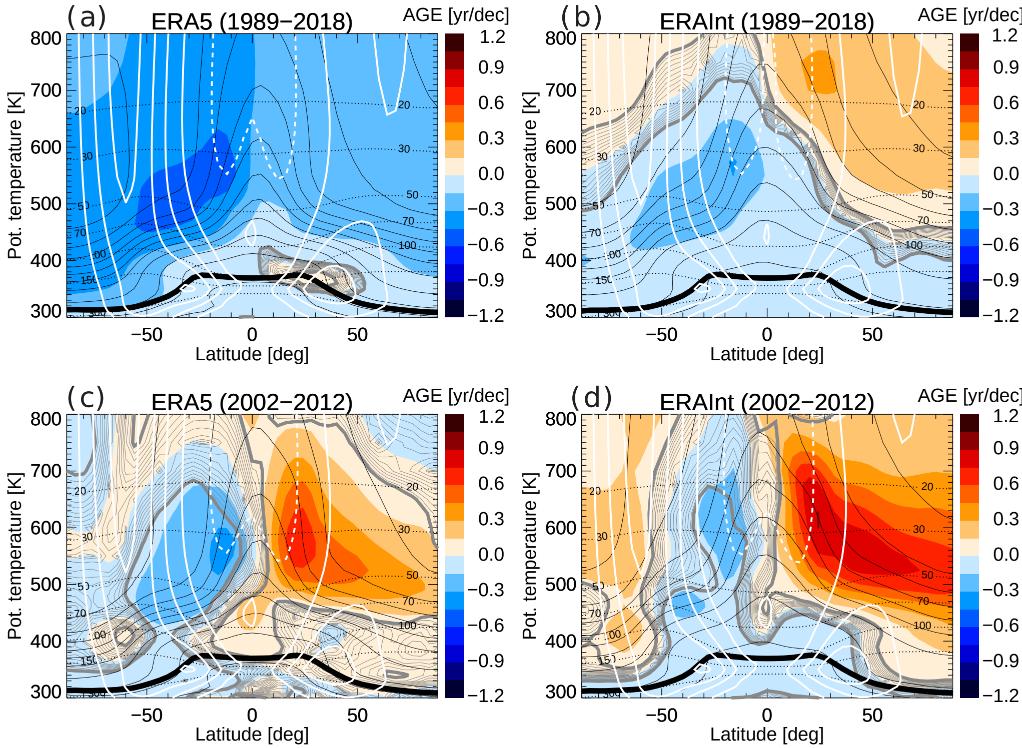

Figure 6. Mean age trends for the period 1989–2018 from ERA5 (a) and ERA–Interim (b). (c–d) Same, but for the 2002–2012 period. Black contours (solid) show climatological mean age, thin dashed black lines pressure levels, white contours zonal wind (in ± 10 m/s steps; easterly wind dashed), and the thick black line the tropopause. The significance of the linear trend, measured in multiples of the standard deviation σ, is shown as gray contours (2 σ contour as thick, then decreasing with 0.2 step as thin lines).

ERA5 is at about 4 years, while for ERA–Interim modal age occurs at 1.4 years. Hence, there is a significantly higher fraction of young air at high latitudes for ERA–Interim than for ERA5.

Similar conclusions hold for the age spectrum comparison at 600 K (Fig. 5). While the general spectrum characteristics are similar for ERA5 and ERA–Interim, clear detailed differences occur in the spectrum shape. ERA5 spectra are shifted towards older transit times and show an older peak compared to ERA–Interim, as found similarly at the lower 400 K level. In the tropics, these differences are particularly clear with the shift of the spectrum peak to older ages in ERA5 compared to ERA–Interim indicating slower residual circulation upwelling ~~(e.g., Li et al., 2012; Ploeger et al., 2019)~~(e.g., Li et al., 2012; Ploeger and Birner, 2016). This slower residual circulation upwelling is consistent with the weaker diabatic heating rates in the TTL and lower tropical stratosphere in Fig. 1. Moreover, the larger extent of the youngest spectrum peak towards high latitudes in the summer hemisphere (e.g., in the NH during JJA ~~,~~in Fig. 5b, and in the SH during DJF in Fig. 5c) shows faster transport of young air towards the pole in ERA–Interim than in ERA5.

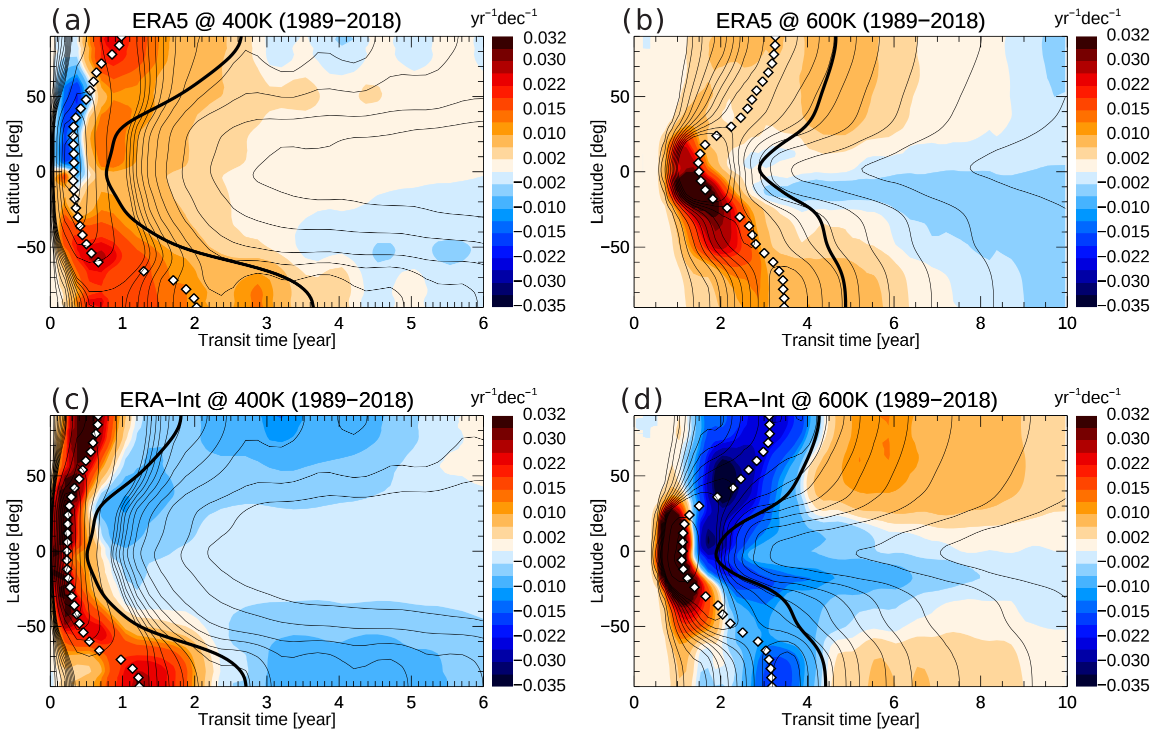

Figure 7. Age spectrum trend for the period 1989–2018 from ERA5 at 400 K (a), and 600 K (c). (c, d) Same, but for ERA–Interim. Thin black contours show annual mean age spectra, thick black contour shows mean age (calculated as first moment of spectra), white diamonds show modal age (peak of the spectrum). Note the different x-axis scales for the two levels.

4 Circulation and age changes over (multi-)decadal time scales

Trends in mean age over the entire 30 year period 1989–2018 and over 2002–2012 are shown in Fig. 6. The trends are calculated from linear regression of the deseasonalized time series (after subtracting the mean annual cycle at each grid point). The standard deviation from the regression provides a 1-σ range for assessing the significance of the calculated trends. Even over 30 years ~~trends~~ trend values are still affected by decadal variability, as will be discussed at the end of this section. Nevertheless, for simplicity we use the term “trend” in this paper but note that our results concern changes over 30 years and not over centennial time scales, as is often the case for climate model experiments.

Evidently, ERA5 shows a negative age trend throughout the stratosphere over the longer period, with strongest decreases of up to -0.5 years per decade (yr/dec) in the SH sub-tropics and mid latitudes. In the SH and in the lowest stratosphere (below about 450 K) this negative age trend qualitatively agrees with the trend from ERA–Interim. In particular in the NH above about 500 K, however, the signs of the trends in the two reanalyses are opposite, with ERA–Interim showing increasing age. These differences will be further discussed in Sect. 6.

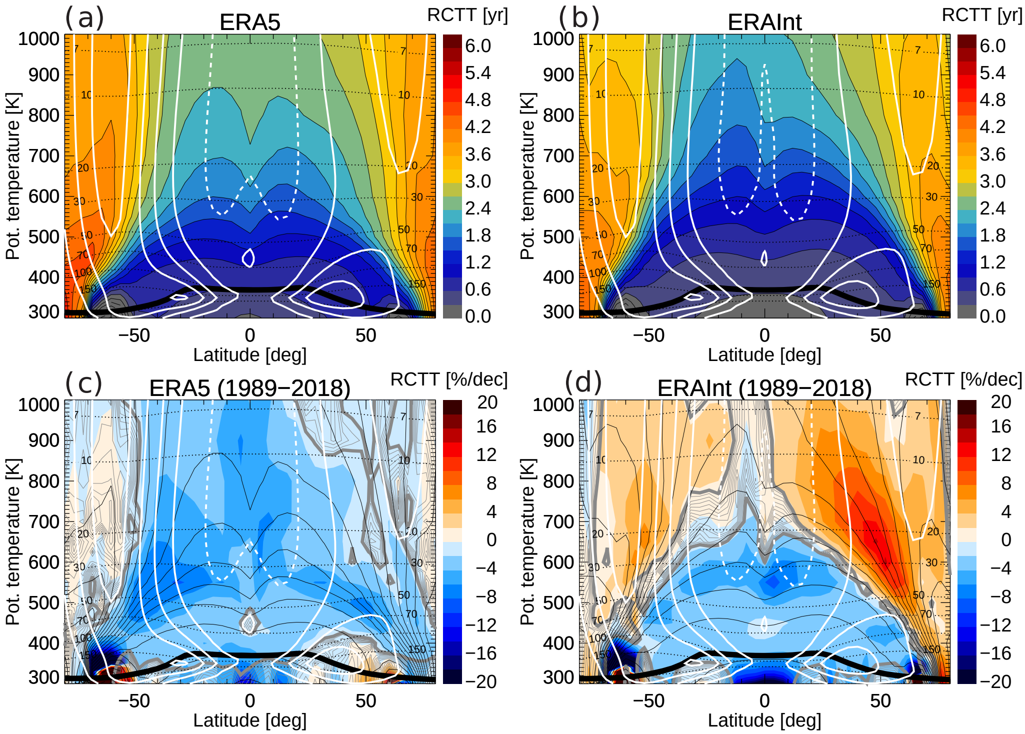

Figure 8. Residual circulation transit times (RCTT) from ERA5 (a) and ERA–Interim (b), and their trends over 1989–2018 (c, d). Thin black lines in c and d show climatological RCTT contours (in 0.3 yr steps). White contours show zonal wind (in ± 10 m/s steps; easterly wind dashed), thin dashed black lines potential temperature levels, the thick black line the (WMO lapse rate) tropopause. The significance of the linear trend, measured in multiples of the standard deviation σ, is shown as gray contours (2 σ contour as thick, then decreasing with 0.2 step as thin lines).

For the shorter period 2002–2012 both reanalyses show qualitatively similar mean age changes, with increasing age in the NH and decreasing age in the SH (Fig. 6c–d). Detailed differences concern a weaker NH age increase and a stronger SH age decrease in ERA5 compared to ERA–Interim. In the lowest tropical and sub-tropical stratosphere ERA5 shows significantly increasing age, although non-significant changes in some regions, compared to decreasing age or insignificant trends in ERA–Interim in this region. Hence, changes in the shallow BDC branch over this short period are not consistent between the two reanalyses. The small quantitative differences for the 2002–2012 ERA–Interim age trends compared to recent publications of CLaMS simulated mean age (e.g., Stiller et al., 2017) are related to the use of clock-tracer versus age spectrum based mean age and to the updates in the model configuration (e.g., exclusion of annual mean cross-isentropic mass balance here)~~and the use of clock-tracer versus age spectrum based mean age~~, as explained in Sect. 2.1.

Trends in the age spectrum provide more detailed information about changes in transport processes and are presented in Fig. 7 for the period 1989–2018 (for the two levels 400 and 600 K). ERA5 age spectra show a shift of the spectrum peak towards younger age for most regions, as indicated by ~~relatively stronger~~ comparatively strong positive spectrum trends at transit times shorter than the modal age (indicating an increase in the mass fraction of young air). Such a decrease of modal age can be interpreted as an acceleration of the residual circulation, at least in the tropics and in the winter hemisphere extratropics ~~(e.g., Li et al., 2012; Ploeger et al., 2019)~~(e.g., Li et al., 2012; Ploeger and Birner, 2016). In the tropics and SH this modal age shift and residual circulation acceleration is clearest. In the NH in a shallow layer around the 400 K level between 0–50°N the age changes are different, with a decrease of the young air fraction (transit times shorter than modal age) causing weak positive mean age changes (compare Fig. 7a and Fig. 6a).

The clearest difference to ERA–Interim regarding structural age spectrum changes emerges at middle and high latitudes at upper levels (here 600 K, Fig. 7b and d). ERA5, on the one hand, shows a shift of the spectrum to younger ages, although not as clear as in the tropics and in the SH. ERA–Interim, on the other hand, shows a decrease in the fraction of air younger than about 4 years and an increase of the fraction of older air. This increased fraction of air older than about 4 years in ERA–Interim indicates a ~~strengthening in~~ deceleration of the deep branch of the residual circulation. The different spectrum changes in ERA5 and ERA–Interim cause the opposite mean age changes in the two reanalyses (Fig. 6), and are related to different trends in the deep BDC branch~~(see next paragraph~~, as evident from further analysis of the residual circulation (see below).

Changes in the structure of the residual circulation are further investigated by using residual circulation transit times (RCTTs), the pure transit time for (hypothetical) air parcels in the 2D residual circulation flow (e.g., Birner and Bönisch, 2011). Here, the RCTTs have been calculated in isentropic coordinates using the same reanalysis diabatic heating rates as in the full CLaMS simulation for calculating vertical motion (e.g., Ploeger et al., 2019). ~~Differences between mean ageand RCTT~~ RCTTs can not be easily compared to mean age, as differences between both quantities are related to mixing effects (e.g., Garny et al., 2014; Dietmüller et al., 2017). Figure 8 shows the climatology and percentage trend in RCTT for the period 1989–2018 for ERA5 and ERA–Interim. Comparison of climatological RCTTs shows substantially longer transit times for ERA5 than ERA–Interim (up to 40% longer in the lower stratosphere), consistent with the slower circulation in ERA5 as already diagnosed from heating rates, $\overline{w}^*$ and age of air. The trends in RCTTs in Fig. 8c–d indicate differences between the reanalyses regarding changes in the structure of the BDC. In the lower stratosphere below about 600 K both reanalyses show consistent changes, with decreasing RCTT indicating a strengthening of the shallow residual circulation branch. In the tropical lower stratosphere the residual circulation accelerates by about 2.4 %/decade in ERA5 and 2.2 %/decade in ERA–Interim, as diagnosed from the RCTT trend (20°N/S, 450 K average, approximately 70 hPa). Clear differences emerge at higher levels and also at higher latitudes, hence in atmospheric regions of the deep circulation branch. In these regions, ERA5 still shows decreasing RCTTs, turning into insignificant changes at high latitudes. ERA–Interim, on the other hand, shows increasing RCTTs, clearest in the NH. Hence, changes in the deep branch of the residual circulation clearly differ between the reanalyses, with a weakly strengthening deep branch in ERA5 and a weakening deep branch in ERA–Interim.

Figure 9 provides further insights into the temporal evolution of mean age at three different locations in the stratosphere. The three locations have been chosen to be representative for the tropical lower stratosphere, and the NH and SH subtropical stratosphere regions of strong mean age trends (compare with Fig. 6). In the tropical lower stratosphere (450 K and 10°S/N; Fig. 9a), the relative difference between ERA5 and ERA–Interim is large and the variability in ERA5 mean age is significantly stronger than in ERA–Interim. At the higher levels, the variability in mean age in the two reanalyses is more comparable in magnitude. From a qualitative point of view, the variability is similar at all locations, with coinciding ups and downs in the age time series, e.g. caused by modulations in the BDC related to the Quasi-Biennial Oscillation (QBO) or El Niño Southern Oscillation ENSO (e.g., Calvo et al., 2010; Konopka et al., 2016). A particularly striking feature is the anomalously high mean age following the year 1991, even higher for ERA5 than ERA–Interim. This significant increase in stratospheric mean age in reanalyses has been related to the Mt. Pinatubo eruption in June 1991 (Diallo et al., 2017). A more detailed analysis of mean age variability is left for future studies.

While Fig. 6 suggests a clear decrease in ERA5 mean age throughout the global stratosphere, the time series in Fig. 9 show that this decrease is not a simple linear trend over the 30 years considered. In fact, outside the tropics mean age appears to increase before about 1991 and in both hemispheres, and in the NH also after about the year 2000 (except in the SH), and decreases in between2000. During the nineties mean age decreases in ERA5. These steplike changes are evident in both reanalysesand could be related to . In the early nineties these age changes are likely related to the Pinatubo eruption (i.e. true atmospheric variabilityor) while at the end of the nineties they could be related to changes in the reanalysis assimilation system observing system assimilated by the reanalyses (see Sect. 6, and also Chabrillat et al., 2018). In particular in the NH (Fig. 9c), the negative age trend in ERA5 during 1989–2018 appears to be related to the strongly increased age values at the beginning of the period. Further discussion of these steplike changes in the age of air time series is presented in Sect. 6.

5 Comparison to trace gas observations

Climatological reanalysis mean age at 20 km altitude is compared to mean age from CO_2 and SF_6 trace gas measurements in Fig. 10. Comparison is made to data from in-situ observations onboard the NASA ER–2 aircraft (as compiled by Waugh and Hall, 2002, for a detailed data description see the references therein). It should be noted that we consider this data set as an observational climatological benchmark here, as similarly done in other model comparisons (e.g., Chabrillat et al., 2018; Diallo et al., 2012 , although the ER–2 flights have been carried out during 1992–1997 while the model data in Fig. 10a is a climatology over 1989–2018. In general, uncertainties in observational mean age estimates are related to non-linearities and imperfect knowledge in tropospheric growth rates, sampling issues, chemistry effects, and measurement errors (Waugh and Hall, 2002). Mean age deduced from observed SF_6 is higher than mean age deduced from CO_2, consistent with the existence of a significant SF_6 chemical sink in the mesosphere (Ray et al., 2017). The latitudinal age distribution in ERA–Interim agrees well with the in-situ data (best for CO_2-based mean age) while the higher ERA5 mean age values are just at the upper margin of the uncertainty range of the in-situ SF_6-based observations. Recently, Leedham Elvidge et al. (2018) have shown that SF_6 based mean age may be biased high even outside of the polar vortex. On the other hand, the ERA5 age data shows a steeper latitudinal gradient in the subtropics which agrees slightly better with the steep gradient in in-situ observed age compared to ERA–Interim.

Comparison to the NH balloon-borne mean age data set of Engel et al. (2017)Figure 10b presents a comparison of mean age time series in the NH middle stratosphere (model data averaged over 40–50°N, 30–5 hPa) with the balloon-borne observations of Engel et al. (2017). The observational uncertainty range includes uncertainty related to the sampling (representativeness),

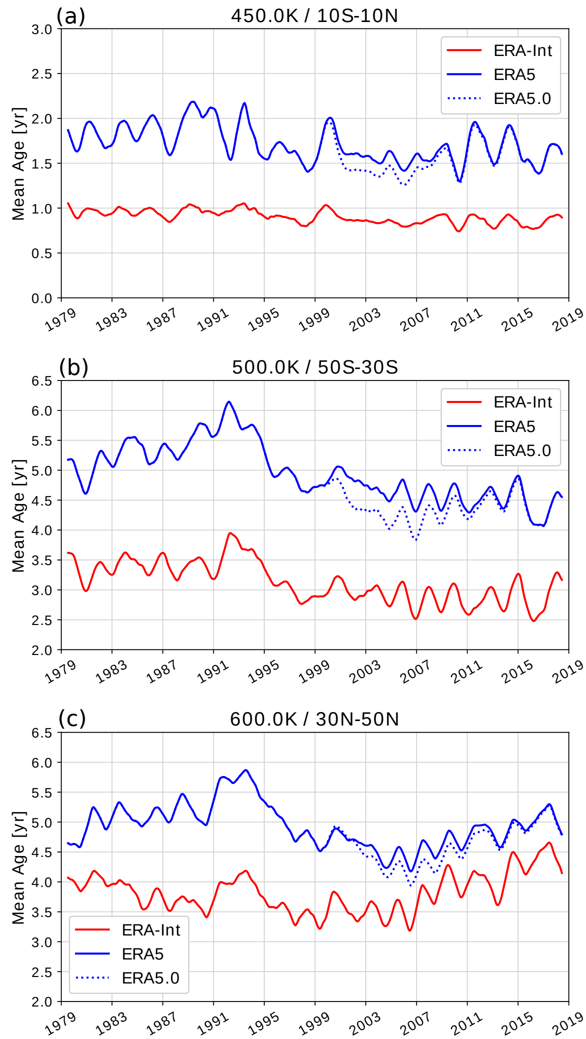

Figure 9. Mean age time series from ERA5 and ERA–Interim in the (a) tropics at 450 K and 10°S–10°N, in the (b) SH subtropics at 500 K and 30–50°S, and in the (c) SH subtropics at 600 K and 30–50°N. The blue dotted line shows mean age from the sensitivity model simulation driven with the uncorrected ERA5.0 data (see text). Data has been deseasonalized by applying a 12 month running mean.

tropospheric mixing ratios, the used age spectrum parameterization and the absolute measurement error (for details see Engel et al., 2009). The comparison shows again that before about 1997 ERA5 age is at the upper ~~margin~~ edge of the observational uncertainty range~~before about 1997~~, while ERA–Interim is at the lower ~~margin~~ edge (Fig. 10b). Regarding the trend, the more gradual increase in ERA–Interim mean age appears to compare better to the observed data than the temporal evolution of ERA5 mean age. In particular the strong decrease in ERA5 age in the mid-nineties is not present in the observations. Although computing a linear trend for a time series with a ~~step~~ steplike change (like for ERA5) is questionable, for completeness we note the

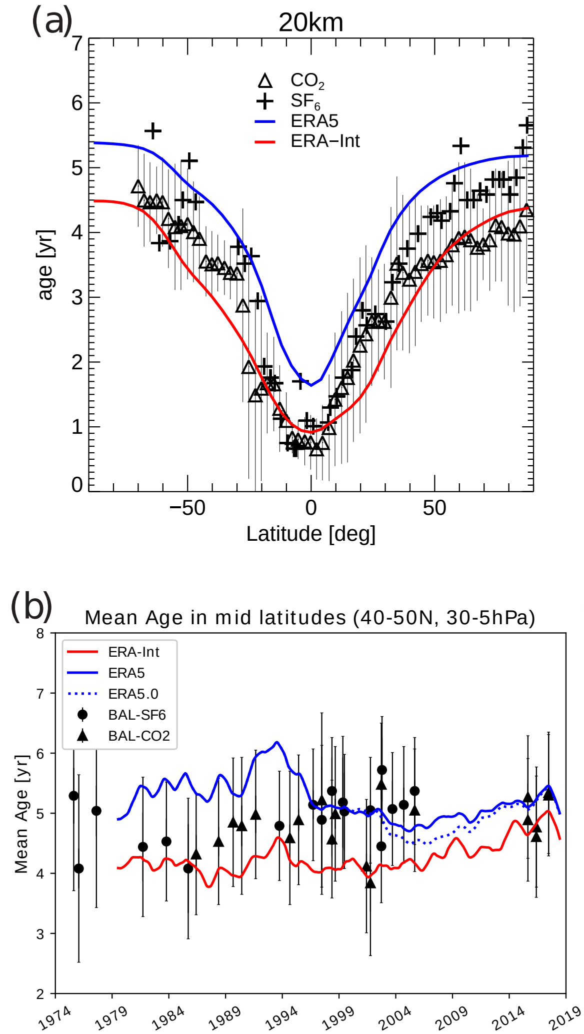

Figure 10. (a) Mean age of air at 20 km at different latitudes from in situ observations (black symbols, from Waugh, 2009), from ERA5 (blue) and ERA–Interim (red) driven CLaMS simulations. (b) Mean age time series in NH middle latitudes (40–50°N and 30–5 hPa, approximately 600–1200 K for reanalyses). Coloured lines show the mean age from reanalyses (smoothed with a 12–month running mean), black symbols show the mean age from the balloon observations of Engel et al. (2017), with error bars representing the uncertainty of the observations.

trend values from a simple linear regression over the period 1989-2018 for ERA5 (-0.13 ± 0.01 years/decade, the error being the 1-σ standard deviation range from the regression) and for ERA–Interim (0.15 ± 0.01 years/decade). The trend value for ERA–Interim agrees with the value stated by Engel et al. (2017), although the observational trend is non-significant. Furthermore, Fritsch et al. (2020) showed recently that the calculated value for the observed mean age trend depends critically on the estimated age spectrum shape, and approaches zero for more recent parameter settings suggested by (Hauck et al., 2019).

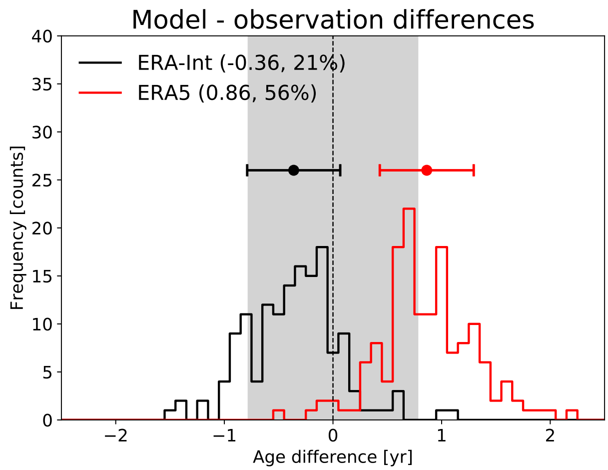

Figure 11. Correlation between CFC–11 and Difference in mean age from between model and Geophysica aircraft observations for ERA5 (greyred) and from ERA–Interim (ablack)ERA5 . Shown are frequency distributions of the mean age differences (bluebin size 0.1 year) and taken in the extratropical lower stratosphere, about 350–480 K (for details on the measurements see Laube et al., 2020). The grey shading shows the mean uncertainty range of the observations (b$\pm$0.78 years)ERA–Interim (, the red and black symbols show the mean differences and the error bars their standard deviation (1-σ) range. Observations The numbers in the legend are from measurement campaigns during 2009–2017 covering the NH lower stratosphere mean difference values (see text for detailsin years) and the percentage of data outside this uncertainty range.

Hence, the comparison between the ERA–Interim and the observed trend value should not be over-interpreted, also given the differences between the single data points of the two time series in Fig. 10b.

Figure ?? 11 further compares the reanalysis mean age to in-situ observations from Geophysica high-altitude aircraft flights in the NH lower stratosphere (for a detailed measurement data description, see Laube et al., 2020). The comparison is done in terms of correlation between CFC–11 and mean age , as similar correlations between mean age and long-lived tracers have been proven beneficial for identifying model transport deficits (e.g., ?). All data sets show the expected negative correlation with lower CFC–11 mixing ratios related to larger age, because of stronger photochemical depletion in older air at upper stratospheric levels. Closer inspection shows that the observations have been taken during five measurement campaigns over 2009–2017 in the NH lower stratosphere (about 350–480 K potential temperature). Mean age has been calculated from measured mixing ratios of CF_4, C_2F_6, C_3F_8, CHF_3 and HFC–125. The observational uncertainty range has been estimated following (Engel et al., 2009), taking into account uncertainties related to non-linearities in tropospheric mixing ratios, age spectrum parameterization and measurement errors, summing up to an overall uncertainty range of $\pm$0.78 years (to be interpreted as 1–σ range). The model output has been sampled along the measurement flight coordinates such that no representativeness errors need to be included. Figure 11 shows the distribution of differences between model and observational mean age for

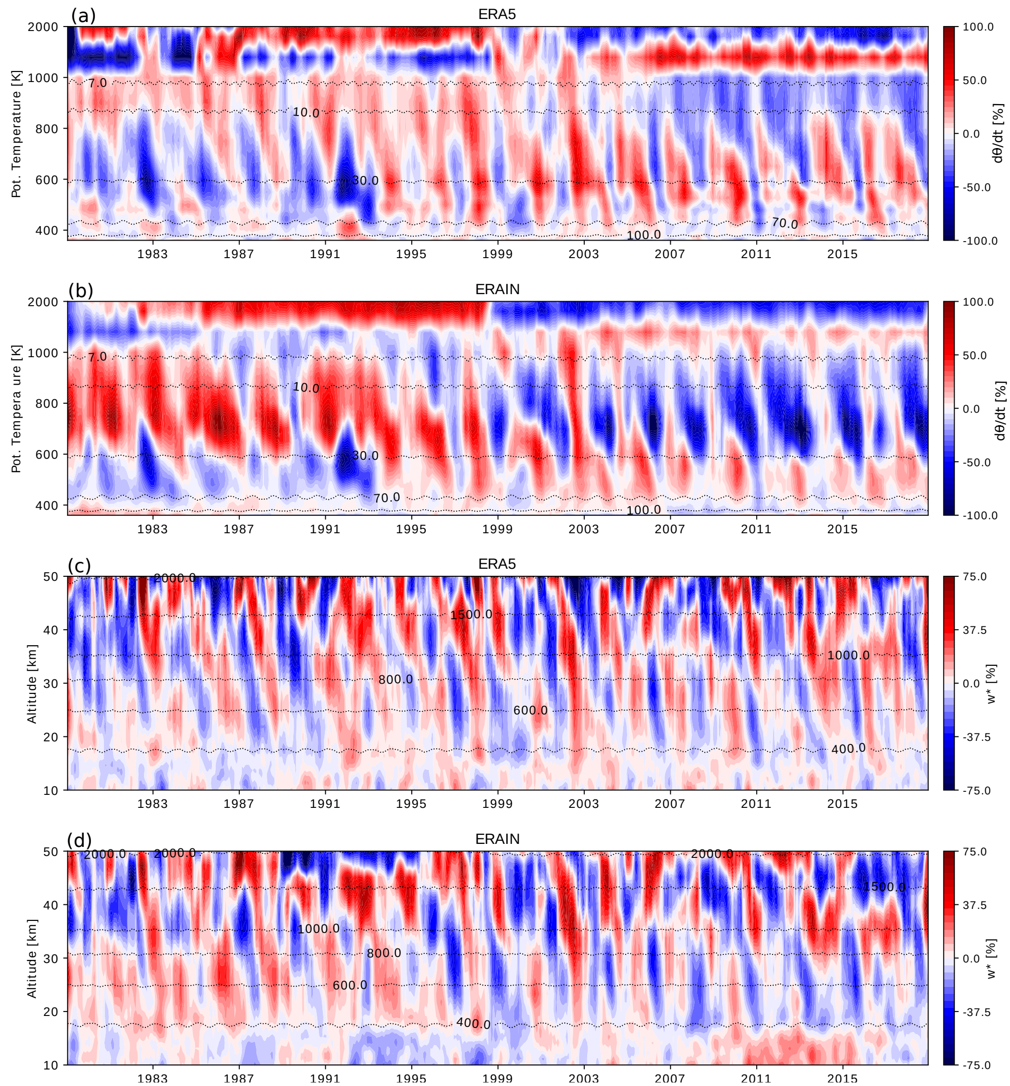

Figure 12. Tropical average monthly mean anomaly time series of total diabatic vertical velocities from ERA5 (a) and ERA–Interim (b), and residual circulation vertical velocity $\overline{w}^*$ from ERA5 (c) and ERA–Interim (d). Data has been averaged over 30°N/S, deseasonalized by subtracting the mean annual cycle, and percentage values have been calculated with respect to the climatological mean. Thin black dashed lines show pressure (a, b) and potential temperature (c, d) levels. Note the scaled potential temperature y-axis above 1000 K (in a, b), to emphasize the lower stratosphere.

mean ages larger than 1 year (to exclude the tropopause region, where the uncertainty in both observational and model mean age is large, related to air entering across the extratropical tropopause). The figure shows that for ERA–Interim the model bias distribution, estimated as the difference between simulated and observed mean age, is largely within the observational uncertainty range (shown as grey shading in Fig. 11, only 21% of data outside this range). For ERA5~~correlation is slightly shifted to the convex side of the observed correlation. This shift can be explained by the slower BDC in~~ , on the other hand, the bias distribution is shifted to mean age differences around 1 year and skewed towards even larger values, such that 56% of the data are outside the observational 1–σ range. Hence, ERA5 ~~compared to ERA–Interim, with air of the same age reaching not as deep into the stratosphere in~~ mean age appears somewhat high-biased in the lower stratosphere. However, the 1–σ ranges of the mean ERA5 ~~and hence experiencing less CFC–11 loss. A qualitatively similar, even stronger, correlation shift was found for MERRA–2 reanalysis by Laube et al. (2020).For the faster BDC in~~ difference (0.43 years, also for ERA–Interim~~the CFC–11 versus age correlation agrees somewhat better with the in-situ observations .~~) and the observational uncertainty overlap (see Fig. 11) and the mean ERA5 bias in age here is not significant at 66% confidence level. Moreover, the considered Geophysica observations are just from five campaigns localized in time and space and it is unclear whether the difference can be considered as a global bias.

6 Discussion

Recent studies have stated a substantial uncertainty in the climatological strength and trends of the stratospheric BDC and age of air in current generation reanalyses (e.g., Abalos et al., 2015; Miyazaki et al., 2016; Chabrillat et al., 2018; Ploeger et al., 2019). Among the considered reanalyses, JRA–55 was shown to have the fastest and MERRA–2 the slowest BDC, with ERA–Interim-based results in between. In the present study, we find the BDC in ERA5 to be significantly slower and age of air significantly higher than in ERA–Interim (e.g., Figs. 1 and 3).

It is so far unclear whether the representation of the BDC in ERA5 is improved compared to the older reanalyses. In the tropical lower stratosphere, the weaker heating rates in ERA5 are consistent with slower residual circulation upwelling found by Diallo et al. (2020) and appear to correct the 30–40% high bias in ERA–Interim heating rates in the tropical tropopause layer (TTL) found in previous studies (e.g., Ploeger et al., 2012; Schoeberl et al., 2012). On the other hand, the minimum in tropical upwelling around the level of zero radiative heating (around 350 K) is much ~~lower~~ more pronounced for ERA5 than for ERA–Interim with heating rates even showing a gap in annual mean upwelling in a shallow layer, similar to the case in MERRA–2 reanalysis (e.g., compare Fig. 1 with Fig. 5 of Ploeger et al., 2019). In a recent paper, Wright et al. (2020) linked differences in reanalysis diabatic heating rates to differences in the representation of clouds. They argued that the upwelling gap in ERA5 and MERRA–2 is likely caused by higher cloud water content in these two reanalyses and related radiative effects. Indeed, seasonal means of ERA5 heating rates show upwelling also at the lower TTL levels, but very confined regionally and much weaker than for ERA–Interim. Hence, while in the tropical lower stratosphere and upper TTL (about 100–50 hPa) the representation of tropical upwelling seems to be improved in ERA5, it is unclear whether the very weak total diabatic heating rates in the ~~lower TTL~~ upper troposphere and lower TTL (200–100 hPa) are realistic.

~~At higher levels in the stratosphere, however,~~ Above the TTL and in the NH stratosphere, age of air in ERA5 is ~~slightly high-biased compared to~~ at the upper edge of the uncertainty range of in-situ observations (Fig. 10a). ~~In the lower stratosphere outside the tropics, a shift in the ERA5 CFC–11/age correlation with respect to aircraft and balloon~~ In particular in the NH lower stratosphere, comparison to Geophysica aircraft in-situ observations ~~further indicates that the BDC in~~ from Laube et al. (2020) shows that ERA5 ~~is somewhat too slow compared to observations~~ mean age is somewhat high-biased and the ERA5 BDC somewhat too slow (Fig. ~~??). It should be noted that these differences are small and that from our analysis the slow BDC in ERA5 is not necessarily incompatible with mean age observations, when taking all uncertainties into account. However, the~~ 11). Hence, all comparisons to observational data presented here indicate that the slow ERA5 BDC is ~~clearly~~ at the upper margin of the observational uncertainty range. However, these differences are not significant due to the large observational uncertainty range and due to the fact that the considered observations are highly localized in time and space. Hence, it is unclear whether the high age and slow BDC in ERA5 represents a global bias.

Comparison of age of air trends shows a similar hemispheric dipole pattern over the 2002–2012 period for ERA5 as for ERA–Interim, which was argued by Stiller et al. (2017) to agree qualitatively with the structural circulation change observed by MIPAS. This observed increase of age in the NH and decrease of age in the SH has so far not been found for "non-ECMWF" reanalyses (Chabrillat et al., 2018; Ploeger et al., 2019). Regarding the long-term trend in the NH, ERA5 and ERA–Interim show differences. While ERA–Interim shows weakly increasing age of air, more consistent with non-significant trend ~~vaues~~ values from balloon-borne in-situ observations (Engel et al., 2017; Fritsch et al., 2020), ERA5 shows decreasing age. ~~Hence, overall~~ Overall, the agreement to stratospheric age of air observations appears slightly better for ERA–Interim compared to ERA5, but with both reanalyses within the observational uncertainty range.

The globally negative age of air trend in ERA5 over 1989–2018 agrees qualitatively with results from climate model simulations, showing an accelerating BDC and decreasing mean age over multi-decadal time scales in response to increasing greenhouse gas ~~con- centrations~~concentrations. In the tropical lower stratosphere, the residual circulation upwelling increase of 2.4 %/dec in ERA5, as inferred from RCTTs, agrees even quantitatively with climate model predictions of 2–3 %/dec (e.g., Butchart, 2014). In the lower tropical stratosphere the residual circulation acceleration in ERA–Interim is similar (see Sect. 4). However, in ERA5 this ~~residual circulation acceleration~~ acceleration of the residual circulation reaches substantially higher whereas in ERA–Interim the deep BDC branch decelerates (Fig. 8).

In a recent study, Diallo et al. (2020) compared the residual circulation in ERA5 and ERA–Interim based on residual circulation vertical velocity $\overline{w}^*$ and stream function. They showed, using these standard circulation metrics, that the BDC in ERA5 is significantly slower than in ERA–Interim, consistent with the findings here based on age of air and the diabatic circulation (heating rate based). Furthermore, they related the weaker residual circulation to weaker gravity wave drag at the upper flanks of the subtropical jets in ERA5 compared to ERA–Interim. Also differences in trends in $\overline{w}^*$ were shown to be likely caused by differences in gravity wave drag. Given the qualitatively similar results between age of air and residual circulation regarding both the weaker climatological BDC and more negative trends in ERA5, it seems likely that reanalysis differences between ERA5 and ERA–Interim in age of air are mainly caused by the differences in residual circulation and that mixing differences play only an amplifying role (as suggested for different data by Garny et al., 2014). The clear differences in the age spectrum peaks (modal ages, compare Figs. 4, 5, 7) corroborate the idea that residual circulation differences cause the mean age differences. An investigation of mixing in ERA5 based on computation of effective diffusivity (e.g., Haynes and Shuckburgh, 2000), as has been realized for other reanalyses recently (e.g., Abalos et al., 2017), could shed more light on the role of mixing processes for age of air differences between the reanalyses.

A closer look shows that the decrease of mean age in ERA5 is not simply linear, particularly in the NH. Mean age time series show even weak increases before about 1991 and after about 2000 and a decrease in between. Although these steplike changes are also visible in ERA–Interim, to some degree, they are much more distinct in ERA5. Whether It is unclear whether these changes in mean age can be explained by known factors of multi-annual to decadal variabily or variability or whether they are related to changes in the observations included in the reanalysis assimilation systemneeds to be shown in future studies. To investigate potential discontinuities in the reanalysis, Fig. 12 presents tropical mean (30°N/S) anomaly time series for total diabatic vertical velocity and residual circulation vertical velocity $\overline{w}^*$. Above about 1000 K potential temperature (about 7 hPa), a clear discontinuity in heating rates in 1998 is evident for both reanalysis, as related for ERA–Interim to the change from TOVS to ATOVS radiance data already by Abalos et al. (2015). For ERA5, this discontinuity appears less pronounced, but is still observable. In the lower stratosphere (below about 1000 K or 10 hPa), however, the heating rate time series indicate no discontinuities. The $\overline{w}^*$ time series show now discontinuities over the entire vertical range and the 1979–2018 period. Hence, we find no indication for sudden changes in the assimilation to cause the steplike change in lower stratospheric age of air in the mid-nineties. If

A very prominent signal in the lower stratosphere (below about 800 K, 10 hPa) is the negative heating rate anomaly during 1991–1992, following the Pinatubo eruption (and similarly in 1982–1983 after the El Chichon eruption). This weakening of tropical upwelling heating rates is even stronger for ERA5 compared to ERA–Interim and is related to the positive mean age anomaly during that period (Fig. 9, and see also Diallo et al., 2017). Hence, the apparent steplike age change in the mid-nineties appears related to the significant age increase (BDC slow-down) after the Pinatubo eruption, in addition to a positive age trend over the eighties in ERA5. Likely, differences between the reanalyses are partly related to differences in the representation of the effect of volcanic aerosol on the BDC. Notably, the response of $\overline{w}^*$ to volcanic eruptions (here Pinatubo, El Chichon) shows positive anomalies (increased tropical upwelling) and is opposite to the heating rate response (see Fig. 12), as already noted for the older reanalysis products in previous studies (e.g., Abalos et al., 2015; Diallo et al., 2017). This difference in the volcanic response in heating rates and residual circulation velocity $\overline{w}^*$ is an important issue for future research, particularly in view of its impact on decadal age of air (and BDC) trends.

If indeed related to real variability, these decadal variations strongly overly in the BDC are significant compared to the potential long-term trend, with even stronger impact in ERA5 in the extratropical stratospherethan ERA–Interim. The 30-40 years time series is presumably still too short for computing long-term trends in reanalysis, where stratospheric variability might be larger compared to climate models. But studying variability on shorter time scales (e.g., inter-annual, decadal) in reanalysis is of value in itself. Whether the long-term mean age trend in ERA5 reanalysis is indeed negative needs to be further analyzed in the future by including more years after 2018, and also before 1979 (as available from an extended ERA5 data product to be released soon).

As mentioned already in Sect. 2.2, we carried out CLaMS model simulations also with the preceding data set with an existing bias in stratospheric temperatures (termed ERA5.0 here). Mean age time series from this sensitivity simulation are included in Figs. 9 and 10 (dotted blue lines). The comparison between ERA5 and ERA5.0 shows that the bias correction indeed has a significant effect on the stratospheric BDC. Without the correction, mean age values suddenly decrease around the year 2000 and remain lower during the following years compared to the corrected ERA5 data. Therefore, in ERA5.0 the steplike age change is even stronger than in the corrected data. Consequently, trends over periods beginning during 2000–2010 (depending on the region under consideration) are more strongly positive for ERA5.0 compared to the corrected ERA5 data. Furthermore, the reduction of the steplike change in age due to the temperature bias correction raises the question whether the remaining steplike change could, at least partly, be related to an incomplete bias correction in ERA5 or to the bias correction starting too late.

As explained in Sect. 2 the CLaMS model simulations are based on the diabatic circulation in the reanalysis as driven by the reanalysis diabatic heating rate. For ERA–Interim it has been shown that the choice of a diabatic versus kinematic transport representation could indeed change the simulated BDC to some degree, in particular regarding trends over decadal periods (Chabrillat et al., 2018; Ploeger et al., 2019). Hence, comparison of the diabatic results here to a similar model study focussing on the ERA5 BDC using a kinematic transport model would be particularly interesting. Furthermore, the present study is based on ERA5 data with full vertical but truncated 1×1 degree horizontal resolution, as provided by ECMWF (see Sect. 2.2). We assume that differences in the global scale BDC patterns caused by the truncation of horizontal resolution, and hence small-scale mixing processes, will be minor. However, at this stage this is just an assumption and can not be proved as full CLaMS simulations with full ERA5 resolution over the entire ERA5 period are so far not feasible due to the excessive amount of reanalysis data needed and necessary further model developments regarding the data handling.

7 Conclusions

We investigated the global stratospheric Brewer-Dobson circulation in the ECMWF ERA5 reanalysis based on age of air simulations with the Lagrangian chemistry transport model CLaMS driven by reanalysis winds and diabatic heating rates. The simulations include both mean age as well as the age of air spectrum. Results are compared against results based on the predecessor reanalysis ERA–Interim.

We find that the global structure and seasonality in both reanalyses is very similar. However, the BDC is substantially slower and age of air larger in ERA5 than in ERA–Interim. In the tropical lower stratosphere and in the upper TTL the 30-40% weaker heating rates in ERA5 appear to correct the too-strong vertical upwelling in ERA–Interim found in previous studies. At higher stratospheric levels above the TTL and in the NH, on the other hand, ERA5 mean age is found to be at the upper margin of the observational uncertainty range.

The mean age trend over the 1989–2018 period in ERA5 is globally negative, as expected from climate model simulations as response to increasing greenhouse gas concentrations. However, outside the tropics the ERA5 mean age decrease is not linear over the entire period but largely related to a steplike change ~~around the year 2000.~~ in the mid-nineties. Hence, it is unclear whether the negative age trend in the reanalysis can be interpreted as response to climate change or is related to decadal variability or changes in the observations included in the data assimilation system. From the absence of sudden changes in heating rate and residual circulation velocity time series the relation to variability, in particular caused by volcanic aerosol, seems more likely, but effects from the assimilation can not be ruled out. Due to the slowness of the circulation and the existence of a negative age trend in the NH the discrepancy with balloon-borne ~~observations is greater~~ and aircraft in-situ observations is larger for ERA5 than ERA–Interim. The mean age change over 2002–2012 in ERA5 shows a similar hemispheric asymmetry pattern as found for ERA–Interim.

Overall, the new ERA5 reanalysis appears promising for transport studies of the BDC. It is certainly important for such studies to use the bias-corrected data set (termed ERA5.1 in ECMWF's documentation). However, whether the representation of stratospheric transport is indeed improved compared to ERA–Interim reanalysis is, so far, unclear.

Data availability. ERA5 and ERA–Interim reanalysis data is available from the ECMWF. The CLaMS model data used for this paper may be requested from the corresponding author (f.ploeger@fz-juelich.de)

Author contributions. FP carried out the CLaMS simulations and the respective analysis, with help from PK, and wrote the manuscript. MD, JUG and GG downloaded and prepared the ERA5 reanalysis data, with advice from BL. EC contributed to the analysis of the model output. JL and AE prepared and provided observational data. All authors contributed to finalizing the manuscript.

Competing interests. The authors declare no competing interests.

Acknowledgements. We are particularly grateful to Nicole Thomas for programming support and help with setting up the CLaMS model simulations with the new ERA5 reanalysis. We further thank Rolf Müller for comments on an earlier version of the manuscript, ~~and~~ the ECMWF for providing reanalysis data, and Simon Chabrillat and an anonymous reviewer for their comments on the submitted manuscript version. This study was funded by the Helmholtz Association under grant no. VH-NG-1128 (Helmholtz Young Investigators Group A–SPECi). Finally, we gratefully acknowledge the computing time for the ~~EMAC~~ CLaMS simulations which was granted on the supercomputer JURECA at the Jülich Supercomputing Centre (JSC) under the VSR project ID JICG11.

References

Abalos, M., Legras, B., Ploeger, F., , and Randel, W. J.: Evaluating the advective Brewer-Dobson circulation in three reanalyses for the period 1979-2012, J. Geophys. Res., 120, 7534–7554, https://doi.org/10.1002/2015JD023182, 2015.

Abalos, M., Shuckburgh, E., and Legras, B.: Interannual variability in effective diffusivity in the upper troposphere/lower stratosphere from reanalysis data, Q. J. R. Meteorol. Soc., 142, 1847–1861, https://doi.org/10.1002/qj.2779, 2017.

Andrews, D. G., Holton, J. R., and Leovy, C. B.: Middle Atmosphere Dynamics, Academic Press, San Diego, USA, 1987.

Birner, T. and Bönisch, H.: Residual circulation trajectories and transit times into the extratropical lowermost stratosphere, Atmos. Chem. Phys., 11, 817–827, https://doi.org/10.5194/acp-11-817-2011, 2011.

Bönisch, H., Engel, A., Curtius, J., Birner, T., and Hoor, P.: Quantifying transport into the lowermost stratosphere using simultaneous in-situ measurements of SF_6 and CO_2, Atmos. Chem. Phys., 9, 5905–5919, 2009.

Butchart, N.: The Brewer-Dobson circulation, Rev. Geophys., 52, 157–184, https://doi.org/10.1002/2013RG000448, 2014.

Butchart, N., Cionni, I., Eyring, V., Shepherd, T., Waugh, D., Akiyoshi, H., Austin, J., Brühl, C., Chipperfield, M., Cordero, E., Dameris, M., Deckert, R., Dhomse, S., Frith, S., Garcia, R., Gettelman, A., Giorgetta, M., Kinnison, D., Li, F., Mancini, E., McLandress, C., Pawson, S., Pitari, G., Plummer, D., Rozanov, E., Sassi, F., Scinocca, J., Shibata, K., Steil, B., and Tian, W.: Chemistry-climate model simulations of 21st century stratospheric climate and circulation changes, J. Climate, 23, 5349–5374, https://doi.org/10.1175/2010JCL13404.1, 2010.

Calvo, N., Garcia, R. R., Randel, W. J., and Marsh, D.: Dynamical mechanism for the increase in tropical upwelling in the lowermost tropical stratosphere during warm ENSO events, J. Atmos. Sci., 67, 2331–2340, https://doi.org/10.1175/2010JAS3433.1, 2010.

Chabrillat, S., Vigouroux, C., Christophe, Y., Engel, A., Errera, Q., Minganti, D., Monge-Sanz, B. M., Segers, A., and Mahieu, E.: Comparison of mean age of air in five reanalyses using the BASCOE transport model, Atmospheric Chemistry and Physics, 18, 14 715–14 735, https://doi.org/10.5194/acp-18-14715-2018, 2018.

Charlesworth, E. J., Dugstad, A.-K., Fritsch, F., Jöckel, P., and Plöger, F.: Impact of Lagrangian Transport on Lower-Stratospheric Transport Time Scales in a Climate Model, Atmos. Chem. Phys., 20, 15 227–15 245, https://doi.org/10.5194/acp-20-15227-2020, 2020.

Dee, D. P., Uppala, S. M., Simmons, A. J., Berrisford, P., Poli, P., Kobayashi, S., Andrae, U., Balmaseda, M. A., Balsamo, G., Bauer, P., Bechtold, P., Beljaars, A. C. M., van de Berg, L., Bidlot, J., Bormann, N., Delsol, C., Dragani, R., Fuentes, M., Geer, A. J., Haimberger, L., Healy, S. B., Hersbach, H., Holm, E. V., Isaksen, L., Kallberg, P., Koehler, M., Matricardi, M., McNally, A. P., Monge-Sanz, B. M., Morcrette, J.-J., Park, B.-K., Peubey, C., de Rosnay, P., Tavolato, C., Thepaut, J.-N., and Vitart, F.: The ERA-Interim reanalysis: configuration and performance of the data assimilation system, Q. J. R. Meteorol. Soc., 137, 553–597, https://doi.org/10.1002/qj.828, 2011.

Diallo, M., Legras, B., and Chédin, A.: Age of stratospheric air in the ERA-Interim, Atmos. Chem. Phys., 12, 12 133–12 154, https://doi.org/10.5194/acp-12-12133-2012, 2012.

Diallo, M., Ploeger, F., Konopka, P., Birner, T., Müller, R., Riese, M., Garny, H., Legras, B., Ray, E., Berthet, G., and Jegou, F.: Significant contributions of volcanic aerosols to decadal changes in the stratospheric circulation, Geophys. Res. Lett., 12, 10 780–10 791, 2017.

Diallo, M., Ern, M., and Ploeger, F.: The advective Brewer-Dobson circulation in the ERA5 reanalysis: variability and trends, Atmos. Chem. Phys., 2020, 1–39, https://doi.org/10.5194/acp-2020-881, 2020.

Dietmüller, S., Garny, H., Plöger, F., Jöckel, P., and Cai, D.: Effects of mixing on resolved and unresolved scales on stratospheric age of air, Atmos. Chem. Phys., 17, 7703–7719, https://doi.org/10.5194/acp-17-7703-2017, 2017.

Engel, A., Möbius, T., Bönisch, H., Schmidt, U., Heinz, R., Levin, I., Atlas, E., Aoki, S., Nakazawa, T., Sugawara, S., Moore, F., Hurst, D., Elkins, J., Schauffler, S., Andrews, A., and Boering, K.: Age of stratospheric air unchanged within uncertainties over the past 30 years, Nature Geoscience, 2, 28–31, https://doi.org/10.1038/ngeo388, 2009.

Engel, A., Bönisch, H., Ullrich, M., Sitals, R., Membrive, O., Danis, F., and Crevoisier, C.: Mean age of stratospheric air derived from AirCore observations, Atmos. Chem. Phys., 17, 6825–6838, https://doi.org/10.5194/acp-17-6825-2017, 2017.

Fritsch, F., Garny, H., Engel, A., Bönisch, H., and Eichinger, R.: Sensitivity of age of air trends to the derivation method for non-linear increasing inert SF_6, Atmos. Chem. Phys., 20, 8709–8725, https://doi.org/10.5194/acp-20-8709-2020, 2020.

Fujiwara, M., Wright, J. S., Manney, G. L., Gray, L. J., Anstey, J., Birner, T., Davis, S., Gerber, E. P., Harvey, V. L., Hegglin, M. I., Homeyer, C. R., Knox, J. A., Krüger, K., Lambert, A., Long, C. S., Martineau, P., Molod, A., Monge-Sanz, B. M., Santee, M. L., Tegtmeier, S., Chabrillat, S., Tan, D. G. H., Jackson, D. R., Polavarapu, S., Compo, G. P., Dragani, R., Ebisuzaki, W., Harada, Y., Kobayashi, C., McCarty, W., Onogi, K., Pawson, S., Simmons, A., Wargan, K., Whitaker, J. S., and Zou, C.-Z.: Introduction to the SPARC Reanalysis Intercomparison Project (S-RIP) and overview of the reanalysis systems, Atmospheric Chemistry and Physics, 17, 1417–1452, https://doi.org/10.5194/acp-17-1417-2017, 2017.

Garny, H., Birner, T., Bönisch, H., and Bunzel, F.: The effects of mixing on Age of Air, J. Geophys. Res., 119, https://doi.org/10.1002/2013JD021417, 2014.

Gelaro, R., McCarty, W., Suárez, M. J., Todling, R., Molod, A., Takacs, L., Randles, C. A., Darmenov, A., Bosilovich, M. G., Reichle, R., Wargan, K., Coy, L., Cullather, R., Draper, C., Akella, S., Buchard, V., Conaty, A., da Silva, A. M., Gu, W., Kim, G.-K., Koster, R., Lucchesi, R., Merkova, D., Nielsen, J. E., Partyka, G., Pawson, S., Putman, W., Rienecker, M., Schubert, S. D., Sienkiewicz, M., and Zhao, B.: The Modern-Era Retrospective Analysis for Research and Applications, Version 2 (MERRA-2), jci, 30, 5419–5454, 2017.

Haenel, F., Stiller, G. P., von Clarmann, T., Funke, B., Eckert, E., Glatthor, N., Grabowski, U., Kellmann, S., Kiefer, M., Linden, A., and Reddmann, T.: Reassessment of MIPAS age of air trends and variability, Atmos. Chem. Phys., 22, 13 161–13 176, https://doi.org/10.5194/acp-15-13161-2015, 2015.

Hall, T. M. and Plumb, R. A.: Age as a diagnostic of stratospheric transport, J. Geophys. Res., 99, 1059–1070, 1994.

Hauck, M., Fritsch, F., Garny, H., and Engel, A.: Deriving stratospheric age of air spectra using an idealized set of chemically active trace gases, Atmos. Chem. Phys., 19, 5269–5291, https://doi.org/10.5194/acp-19-5269-2019, 2019.

Haynes, P. and Shuckburgh, E.: Effective diffusivity as a diagnostic of atmospheric transport, 1, Stratosphere, J. Geophys. Res., 105, 22 777–22 794, 2000.

Haynes, P. H., Marks, C. J., McIntyre, M. E., Shepherd, T. G., and Shine, K. P.: On the “downward control” of extratropical diabatic circulations by eddy-induced mean zonal forces., J. Atmos. Sci., 48, 651–678, 1991.

Hegglin, M. I. and Shepherd, T. G.: O_3-N_2O correlations from the Atmospheric Chemistry Experiment: Revisiting a diagnostic of transport and chemistry in the stratosphere, J. Geophys. Res., D19301, https://doi.org/10.1029/2006JD008281, 2007.

Hersbach, H., Bell, B., Berrisford, P., Hirahara, S., Horanyi, A., Munoz-Sabater, J., Nicolas, J., Peubey, C., Radu, R., Schepers, D., Simmons, A., Soci, C., Abdalla, S., Abellan, X., Balsamo, G., Bechtold, P., Biavati, G., Bidlot, J., Bonavita, M., De Chiara, G., Dahlgren, P., Dee, D., Diamantakis, M., Dragani, R., Flemming, J., Forbes, R., Fuentes, M., Geer, A., Haimberger, L., Healy, S., Hogan, R. J., Hólm, E., Janiskova, M., Keeley, S., Laloyaux, P., Lopez, P., Lupu, C., Radnoti, G., de Rosnay, P., Rozum, I., Vamborg, F., Villaume, S., and Thepaut, J.-N.: The ERA5 global reanalysis, Q. J. R. Meteorol. Soc., 146, 1999–2049, https://doi.org/https://doi.org/10.1002/qj.3803, 2020.

Holton, J. R., Haynes, P., McIntyre, M. E., Douglass, A. R., Rood, R. B., and Pfister, L.: Stratosphere-troposphere exchange, Rev. Geophys., 33, 403–439, 1995.

Kobayashi, S., Ota, Y., Harada, Y., Ebita, A., Moriya, M., Onoda, H., Onogi, K., Kamahori, H., Kobayashi, C., Endo, H., Miyaoka, K., and Takahashi, K.: The JRA–55 Reanalysis: General specifications and basic characteristics, J. Meteorol. Soc. Jpn., 93, 5–48, 2015.

Konopka, P., Steinhorst, H.-M., Grooß, J.-U., Günther, G., Müller, R., Elkins, J. W., Jost, H.-J., Richard, E., Schmidt, U., Toon, G., and McKenna, D. S.: Mixing and Ozone Loss in the 1999-2000 Arctic Vortex: Simulations with the 3-dimensional Chemical Lagrangian Model of the Stratosphere (CLaMS), J. Geophys. Res., 109, D02315, https://doi.org/10.1029/2003JD003792, 2004.

Konopka, P., Grooß, J.-U., Günther, G., Ploeger, F., Pommrich, R., Müller, R., and Livesey, N.: Annual cycle of ozone at and above the tropical tropopause: observations versus simulations with the Chemical Lagrangian Model of the Stratosphere (CLaMS), Atmos. Chem. Phys., 10, 121–132, https://doi.org/10.5194/acp-10-121-2010, 2010.

Konopka, P., Ploeger, F., Tao, M., and Riese, M.: Zonally resolved impact of ENSO on the stratospheric circulation and water vapor entry values, J. Geophys. Res., 121, 11 486–11 501, https://doi.org/10.1002/2015JD024698, 2016.

Laube, J. C., Elvidge, E. C. L., Adcock, K. E., Baier, B., Brenninkmeijer, C. A. M., Chen, H., Droste, E. S., Grooß, J.-U., Heikkinen, P., Hind, A. J., Kivi, R., Lojko, A., Montzka, S. A., Oram, D. E., Randall, S., Röckmann, T., Sturges, W. T., Sweeney, C., Thomas, M., Tuffnell, E., and Ploeger, F.: Investigating stratospheric changes between 2009 and 2018 with halogenated trace gas data from aircraft, AirCores, and a global model focusing on CFC-11, Atmos. Chem. Phys., 20, 9771–9782, https://doi.org/10.5194/acp-20-9771-2020, 2020.

Leedham Elvidge, E., Bönisch, H., Brenninkmeijer, C. A. M., Engel, A., Fraser, P. J., Gallacher, E., Langenfelds, R., Mühle, J., Oram, D. E., Ray, E. A., Ridley, A. R., Röckmann, T., Sturges, W. T., Weiss, R. F., and Laube, J. C.: Evaluation of stratospheric age of air from CF_4, C_2F_6, C_3F_8, CHF_3, HFC-125, HFC-227ea and SF_6; implications for the calculations of halocarbon lifetimes, fractional release factors and ozone depletion potentials, Atmos. Chem. Phys., 18, 3369–3385, https://doi.org/10.5194/acp-18-3369-2018, 2018.

Li, D., Vogel, B., R, M., Bian, J., Günther, G., Ploeger, F., Li, Q., Zhang, J., Bai, Z., Vömel, H., and Riese, M.: Dehydration and low ozone in the tropopause layer over the Asian monsoon caused by tropical cyclones: Lagrangian transport calculations using ERA-Interim and ERA5 reanalysis data, Atmos. Chem. Phys., 20, 4133–4152, https://doi.org/10.5194/acp-20-4133-2020, 2020.

Li, F., Waugh, D. W., Douglass, A. R., Newman, P. A., Pawson, S., Stolarski, R. S., Strahan, S. E., and Nielsen, J. E.: Seasonal variations in stratospheric age spectra in GEOSCCM, J. Geophys. Res., 117, D5, https://doi.org/10.1029/2011JD016877, 2012.

Lin, P. and Fu, Q.: Changes in various branches of the Brewer-Dobson circulation from an ensemble of chemistry climate models, J. Geophys. Res., 118, 73–84, https://doi.org/10.1029/2012JD018813, 2013.

Mahowald, N. M., Plumb, R. A., Rasch, P. J., del Corral, J., and Sassi, F.: Stratospheric transport in a three-dimensional isentropic coordinate model, J. Geophys. Res., 107, 4254, https://doi.org/10.1029/2001JD001313, 2002.

McKenna, D. S., Konopka, P., Grooß, J.-U., Günther, G., Müller, R., Spang, R., Offermann, D., and Orsolini, Y.: A new Chemical Lagrangian Model of the Stratosphere (CLaMS): 1. Formulation of advection and mixing, J. Geophys. Res., 107, 4309, https://doi.org/10.1029/2000JD000114, 2002.

Minganti, D., Chabrillat, S., Christophe, Y., Errera, Q., Abalos, M., Prignon, M., Kinnison, D. E., and Mahieu, E.: Climatological impact of the Brewer–Dobson circulation on the N_2O budget in WACCM, a chemical reanalysis and a CTM driven by four dynamical reanalyses, Atmos. Chem. Phys., 20, 12 609–12 631, https://doi.org/10.5194/acp-20-12609-2020, 2020.

Miyazaki, K., Iwasaki, T., Kawatani, Y., Kobayashi, C., Sugawara, S., and Hegglin, M. I.: Inter-comparison of stratospheric mean-meridional circulation and eddy mixing among six reanalysis data sets, Atmos. Chem. Phys., 16, 6131–6152, https://doi.org/10.5194/acp-16-6131-2016, 2016.

Monge-Sanz, B. M., Chipperfield, M. P., Dee, D. P., Simmons, A. J., and Uppala, S. M.: Improvements in the stratospheric transport achieved by a chemistry transport model with ECMWF (re)analyses: identifying effects and remaining challenges, Q. J. R. Meteorol. Soc., 139, 654–673, 2012.

Neu, J. L. and Plumb, R. A.: Age of air in a "leaky pipe" model of stratospheric transport, J. Geophys. Res., 104, 243–255, https://doi.org/10.1029/1999JD900251, 1999.

Ploeger, F. and Birner, T.: Seasonal and inter-annual variability of lower stratospheric age of air spectra, Atmos. Chem. Phys., 16, 10 195–10 213, https://doi.org/10.5194/acp-16-10195-2016, 2016.

Ploeger, F., Konopka, P., Günther, G., Grooß, J.-U., and Müller, R.: Impact of the vertical velocity scheme on modeling transport across the tropical tropopause layer, J. Geophys. Res., 115, D03301, https://doi.org/10.1029/2009JD012023, 2010.

Ploeger, F., Konopka, P., Müller, R., Fueglistaler, S., Schmidt, T., Manners, J. C., Grooß, J.-U., Günther, G., Forster, P. M., and Riese, M.: Horizontal transport affecting trace gas seasonality in the Tropical Tropopause Layer (TTL), J. Geophys. Res., 117, D09303, https://doi.org/10.1029/2011JD017267, 2012.

Ploeger, F., Legras, B., Charlesworth, E., Yan, X., Diallo, M., Konopka, P., Birner, T., Tao, M., Engel, A., and Riese, M.: How robust are stratospheric age of air trends from different reanalyses?, Atmos. Chem. Phys., 19, 6085–6105, https://doi.org/10.5194/acp-19-6085-2019, 2019.

Plumb, R. A.: Stratospheric transport, J. Meteorol. Soc. Jpn., 80, 793–809, 2002.

Pommrich, R., Müller, R., Grooß, J.-U., Konopka, P., Ploeger, F., Vogel, B., Tao, M., Hoppe, C. M., Günther, G., Spelten, N., Hoffmann, L., Pumphrey, H.-C., Viciani, S., D'Amato, F., Volk, C. M., Hoor, P., Schlager, H., and Riese, M.: Tropical troposphere to stratosphere transport of carbon monoxide and long-lived trace species in the Chemical Lagrangian Model of the Stratosphere (CLaMS), Geoscientific Model Development, 7, 2895–2916, https://doi.org/10.5194/gmd-7-2895-2014, 2014.

Ray, E. A., Moore, F. L., Elkins, J. W., Rosenlof, K. H., Laube, J., Röckmann, T., Marsh, D. R., and Andrews, A. E.: Quantification of the SF_6 lifetime based on mesospheric loss measured in the stratospheric polar vortex, J. Geophys. Res., 122, 4626–4638, 2017.

Reithmeier, C., Sausen, R., and Greve, V.: Invstigation lower stratospheric model ttransport: Lagrangian calculations of mean age and age spectra in the GCM ECHAM4, Clim. Dyn., 30:225-238, 2007.

Rosenlof, K. H.: Seasonal cycle of the residual mean meridional circulation in the stratosphere, J. Geophys. Res., 100, 5173 – 5191, 1995.

Schoeberl, M. R., Dessler, A. E., and Wang, T.: Simulation of stratospheric water vapor and trends using three reanalyses, Atmos. Chem. Phys., 12, 6475–6487, https://doi.org/10.5194/acp-12-6475-2012, 2012.

Simmons, A., Soci, C., Nicolas, J., Bell, B., Berrisford, P., Dragani, R., Flemming, J., Haimberger, L., Healy, S., Hersbach, H., Horanyi, A., Inness, A., Munoz-Sabater, J., Radu, R., and Schepers, D.: Global stratospheric temperature bias and other stratospheric aspects of ERA5 and ERA5.1, ECMWF Tech. Mem., https://doi.org/10.21957/rcxqfmg0, 2020.

Stiller, G. P., von Clarmann, T., Haenel, F., Funke, B., Glatthor, N., Grabowski, U., Kellmann, S., Kiefer, M., Linden, A., Lossow, S., and López-Puertas, M.: Observed temporal evolution of global mean age of stratospheric air for the 2002 to 2010 period, Atmos. Chem. Phys., 12, 3311–3331, https://doi.org/10.5194/acp-12-3311-2012, 2012.

Stiller, G. P., Fierli, F., Ploeger, F., Cagnazzo, C., Funke, B., Haenel, F., Reddmann, T., Riese, M., and von Clarmann, T.: Shift of subtropical transport barriers explains observed hemispheric asymmetry of decadal trends of age of air, Atmos. Chem. Phys., 17, 11 177–11 192, 2017.

Waugh, D. W.: The age of stratospheric air, Nature Geoscience, 2, 14–16, 2009.

Waugh, D. W. and Hall, T. M.: Age of stratospheric air: Theory, observations, and models, Rev. Geophys., 40, 1–27, 2002.

Wright, J. S., Sun, X., Konopka, P., Krüger, K., Legras, B., Molod, A. M., Tegtmeier, S., Zhang, G. J., and Zhao, X.: Differences in tropical high clouds among reanalyses: origins and radiative impacts, Atmos. Chem. Phys., 20, 8989–9030, https://doi.org/10.5194/acp-20-8989-2020, 2020.